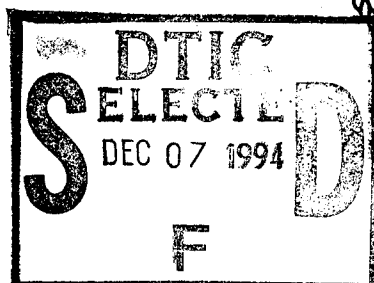# NAVAL POSTGRADUATE SCHOOL
Monterey, California

THESIS

CHARACTERIZATION OF ULTRA-LOW CARBON
BAINTIC STEELS FOR USE AS
WELD WIRE CONSUMABLES

by

Michael L. Beno

September, 1994

Thesis Advisor: Alan G. Fox

19941201 070

DTIC QUALITY INSPECTED 5

REPORT DOCUMENTATION PAGE

Form Approved OMB No. 0704

1. AGENCY USE ONLY	2. REPORT DATE September 1994	3. REPORT TYPE AND DATES COVERED Master's Thesis

4. TITLE AND SUBTITLE: CHARACTERIZATION OF ULTRA-LOW CARBON BAINTIC STEELS FOR USE AS WELD WIRE CONSUMABLES	5. FUNDING NUMBERS DOC # N00167-94-WR-40321 REF # N0001494WX35069
6. AUTHOR(S) Michael L. Beno	

7. PERFORMING ORGANIZATION NAME(S) AND ADDRESS(ES) Naval Postgraduate School Monterey, CA 93943-5000	8. PERFORMING ORGANIZATION REPORT NUMBER

9. SPONSORING/MONITORING AGENCY NAME(S) AND ADDRESS(ES) Naval Surface Warfare Center Carderock Division, Annapolis Detachment Annapolis, MD 21402	10. SPONSORING/MONITORING AGENCY REPORT NUMBER

11. SUPPLEMENTARY NOTES The views expressed in this thesis are those of the author and do not reflect the official policy or position of the Department of Defense or the U.S. Government.

12a. DISTRIBUTION/AVAILABILITY STATEMENT Approved for public release; distribution is unlimited.	12b. DISTRIBUTION CODE *A

13. ABSTRACT

The use of Ultra-Low Carbon Bainitic (ULCB) steels for weld wire applications is an area of current interest to the U. S. Navy and is being jointly studied by the Naval Postgraduate School, and the Naval Surface Warfare Center, Annapolis, MD. The focus of the present work is to determine the effect of macrostructure, microstructure, and the size, distribution and chemical composition of the non-metallic inclusions on the strength and impact toughness of multipass Gas Metal Arc (GMA) and Gas Tungsten Arc (GTA) welds. Eight sample multipass GMA and GTA weldments using ULCB weld wire were studied by optical, scanning electron and transmission electron microscopy (SEM and TEM). The microstructures of the weld metals were dominantly bainitic except for the recrystallized regions of the GTA welds which had become ferritic. The macrostructure of the GMA weldments was dominated by columnar grains. SEM and optical fractography suggested that this macrostructure is responsible for the corresponding poor toughness in these weldments. In all weldments the non-metallic inclusions were found to be very small (on average < 0.5 microns) with a somewhat higher volume fraction in the GMA vice GTA weldments. Based on previous work, the small average size of these inclusions are surmised to have had very little effect on toughness.

14. SUBJECT TERMS Ultra-low Carbon Baintic (ULCB), Toughness, Non-metallic inclusions. Gas Metal Arc Welding Gas Tungsten Arc Welding	15. NUMBER OF PAGES 97
	16. PRICE CODE

17. SECURITY CLASSIFICATION OF REPORT Unclassified	18. SECURITY CLASSIFICATION OF THIS PAGE Unclassified	19. SECURITY CLASSIFICATION OF ABSTRACT Unclassified	20. LIMITATION OF ABSTRACT UL

NSN 7540-01-280-5500

Standard Form 298 (Rev. 2-89)
Prescribed by ANSI STD. 239-18

Approved for public release; distribution is unlimited.

CHARACTERIZATION OF ULTRA-LOW CARBON BAINITIC STEELS FOR USE AS WELD WIRE
CONSUMABLES

by

Michael L. Beno
Lieutenant, United States Navy
B.S., United States Naval Academy, 1988

Submitted in partial fulfillment
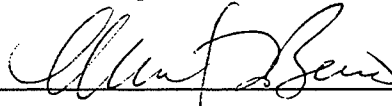of the requirements for the degree of

MASTER OF SCIENCE IN MECHANICAL ENGINEERING

from the

NAVAL POSTGRADUATE SCHOOL
September 1994

Author: _____
Michael L. Beno

Approved by: _____
Alan G. Fox, Thesis Advisor

_____
Matthew D. Kelleher, Chairman
Department of Mechanical Engineering

ABSTRACT

The use of Ultra-Low Carbon Bainitic (ULCB) steels for weld wire applications is an area of current interest to the U. S. Navy and is being jointly studied by the Naval Postgraduate School, and the Naval Surface Warfare Center, Annapolis, MD. The focus of the present work is to determine the effect of macrostructure, microstructure, and the size, distribution and chemical composition of the non-metallic inclusions on the strength and impact toughness of multipass Gas Metal Arc (GMA) and Gas Tungsten Arc (GTA) welds. Eight sample multipass GMA and GTA weldments using ULCB weld wire were studied by optical, scanning electron and transmission electron microscopy (SEM and TEM). The microstructures of the weld metals were dominantly bainitic except for the recrystallized regions of the GTA welds which had become ferritic. The macrostructure of the GMA weldments was dominated by columnar grains. SEM and optical fractography suggested that this macrostructure is responsible for the corresponding poor toughness in these weldments. In all weldments the non-metallic inclusions were found to be very small (on average < 0.5 microns) with a somewhat higher volume fraction in the GMA vice GTA weldments. Based on previous work, the small average size of these inclusions are surmised to have had very little effect on toughness.

iii

Accesion For		
NTIS CRA&I		☑
DTIC TAB		☐
Unannounced		☐
Justification		
By		
Distribution /		
Availability Codes		
Dist	Avail and / or Special	
A-1		

TABLE OF CONTENTS

LIST OF TABLES

LIST OF FIGURES

ACKNOWLEDGEMENTS

I would like to thank my advisor, Dr. Alan Fox for his guidance and assistance in this thesis work. His knowledge of the subject was invaluable and his enthusiasm for his research endless. Also, thanks go to Dr. Michael Vassilaros of NSWC Annapolis, MD for his assistance and research suggestions.

I. INTRODUCTION

Strong, tough, easily fabricated steels have always been the desire of every person involved with ship design or shipbuilding. The U. S. Navy has taken the lead in research in this area in an effort to maximize those three characteristics while minimizing cost and weight. Current production steels in U. S. Navy construction, High Yield 80 (HY-80) and High Yield 100 (HY-100) are strong and relatively tough, but also difficult to fabricate as far as welding is concerned due largely to their high carbon contents. As any object is only as strong as its weakest link, proper welding of these steels is critical.

Recently a new type of steel designated High Strength Low Alloy (HSLA) has come into use for ship construction. While maintaining high strength and impact toughness, HSLA steels are much less difficult to weld owing to their lower carbon content. This eliminates the need for strict control of many welding parameters such as preheat and interpass temperatures. The most effective type of welding process, cover gases, and power inputs are still being researched and are the primary purpose for this work.

Two welding processes, Gas Metal Arc Welding (GMAW or MIG) and Gas Tungsten Arc Welding (GTAW or TIG) on HSLA-100

steel are studied. The weld filler metals were made from Ultra-Low Carbon Bainitic (ULCB) steel. ULCB steels are being considered because of their high strength and toughness owing to their bainitic microstructure. Additionally, the extremely low carbon content serves to reduce the incidence of post weld cracking. The development of ULCB weld wire consumables for use in MIG and TIG welding is the subject of the present research. The macro and microstructure of the welds along with the composition of the non-metallic inclusions are investigated to ascertain their effect on the toughness of the weld. In general, TIG welds are tougher than MIG due to their high degree of grain refinement, but low weld deposition rates motivate the desire for an alternative to TIG welding. MIG welding has a much higher deposition rate of weld metal, but often leaves weaker welds due to a columnar macrostructure. A continuing effort is underway to impart TIG toughness to MIG weldments through control of heat inputs and oxygen content of the weld.

II. BACKGROUND

A. CHARACTERISTICS OF HIGH YIELD AND HIGH STRENGTH LOW ALLOY STEELS

The U. S. Navy has relied on the use of High Yield (HY) steels for many years for all of its ship and submarine construction, and recently has begun to introduce High Strength Low Alloy (HSLA) steel into new programs. HY steels are conventional quenched and tempered martensitic steels which rely on a relatively high carbon content in conjunction with other alloying agents to achieve desired strength and toughness. HSLA steels have a much lower carbon content, and rely on increased alloying agent concentration, specifically copper for precipitation hardening [Garcia, 1991], to achieve the same strength levels as HY steels. Nominal compositions for both HY-100 and HSLA-100 are shown in Table 2.1.

Each of the alloying elements in HY-100 plays an important role in the strength and/or toughness of the steel. Specifically:

●**Carbon** – Hardenability agent. Increased carbon allows for the easier formation of martensite during quenching, and acts as a solid solution strengthener.

●**Manganese** – Solid solution strengthener and toughener. Also combines with sulfur to form MnS before FeS can form. FeS along grain boundaries often leads to lamellar tearing of metal [Abson, 1986].

3

•**Sulfur** - not added intentionally, but present in small amounts in nearly all steels. Removed to less than 0.005 wt% during steel refining to improve resistance to lamellar tearing.

•**Silicon** - Solid solution strengthener, but generally regarded as poor for toughness [Abson, 1986].

•**Nickel** - Hardenability agent which strengthens through grain refinement and solid solution strengthening. Also excellent toughening agent [Abson, 1986].

•**Chromium** - Solid solution strengthener and toughener.

•**Molybdenum** - Solid solution strengthener. Also strong carbide former. Second to carbon in strengthening ability [Abson,1986].

In addition to toughness provided by alloying agents, toughness for HY-100 is achieved through tempering. Tempering is necessary because HY-100 is martensitic after quenching, and without a temper it would be much too brittle. The degree of toughness is controlled by the duration and temperature of the tempering process. Like many other things though, tempering does not increase toughness without consequence, it is increased at the expense of strength.

4

TABLE 2.1 HY-100, HSLA-100, ULCB-100 NOMINAL COMPOSITIONS

	C	Mn	P	S	Si
HY-100	0.17	0.25	0.01	0.005	0.25
HSLA-100	0.04	0.90	0.01	0.005	0.25
ULCB-100	0.02	1.00	–	–	< 0.40

	Ni	Cr	Mo	Cu	Nb
HY-100	2.90	1.40	0.40	0.05	0.00
HSLA-100	3.50	0.60	0.60	1.60	0.03
ULCB-100	2.00	–	1.50 CS 1.00 MV	–	–

HSLA steels take a different route to obtain their strength and toughness. Although they are also quenched and tempered steels, the carbon content is cut by approximately 75% from HY steels which greatly lessens the likelihood of the formation of higher carbon martensite during quenching. This leads to a microstructure of tempered martensite near the surface where cooling rates during the quench are greatest, and tempered bainite elsewhere. In addition to the alloying elements present in HY steels, HSLA steels increase their strength by adding:

●**Niobium** – Strengthens by assisting in carbide and nitride formation specifically niobium carbonitrides. NbCN particles pin prior austenite grain boundaries during hot working and thus lead to small martensite/bainite "packets" which have a high strength and toughness [Wilson, 1991].

5

•**Copper** – Hardenability agent. Strengthens through precipitation hardening [Garcia, 1991].

Copper and niobium make up for the loss in strength normally gained from carbon in high strength steels. NbCN precipitates are especially important as they serve to pin prior austenite grain boundaries during hot working. In addition, the final roll pass for this steel takes place below the recrystalization temperature of austenite introducing dislocations which are then present after transformation to martensite/bainite. The fact that HSLA steels rely for some of their strength on high dislocation densities will prove an important issue in its welding. Toughness in HSLA steels is achieved through the toughening alloying agents and from its basic bainitic/martensitic microstructure which has a small 'packet' size due to the small prior austenite grain size.

The welding of these steels is very important to a ship or submarine as it is only as strong as its weakest point. The difficulty in welding HY steels has been a thorn in the side of shipbuilders since their introduction into Naval construction, and this has led to the development of alternative lower carbon content steels such as HSLA steels. The high carbon content of HY steels make it very easy for brittle martensite to form in regions of the Heat Affected Zone (HAZ) which may have locally higher concentrations of carbon if the cooling rates are not closely controlled. High

6

carbon martensite is very susceptible to Hydrogen Induced Cracking (HIC) as well as having poor toughness characteristics and is thus very undesirable in a steel which may be subject to hydrogen in the welding process or possible rapid changes in loading (impact). Because of these problems, HY steels are always welded with very strict attention paid to parameters such as preheat, interpass temperatures, and heat input in an effort to achieve the desired cooling rate. Proper cooling rates can eliminate the possibility of high carbon martensite, and proper interpass temperatures can act as post-weld tempering for previous weld passes, but the process could be much more cost effective and efficient if these strict controls were not necessary to achieve a high quality weld.

HSLA steels remove the need for much of this strict control by using a much lower carbon content. Lower carbon content leads to less likelihood of high carbon regions which could transform into brittle martensite. This removes the requirement for narrow bands of appropriate cooling rate and gives the welder much greater flexibility in when and how the welding takes place. The point of concern for HSLA steels in welding comes form the loss of dislocation density during the full or partial recrystalization which occurs in most multipass welds.

Carbon equivalent is a measure of the hardenability of a steel and is defined for high strength steels as: $CE = C + (Mn + Si)/6 + (Ni + Cu)/15 + (Cr + Mo + V)/5$ [Czyrka, 1990]. The carbon equivalent for the nominal compositions of both HY-100 and HSLA-100 work out to be the same, 0.81. However, because the actual carbon content is lower in HSLA steels they are easier to weld. Figure 2.1 is the Graville diagram which shows the degree of weldability of steels based on their actual carbon content and carbon equivalent. The advantage of achieving strength through alloying agents rather than carbon in a welding sense is obvious, regardless of the carbon equivalent, the steel remains relatively easy to weld. Of course there is a drawback to achieving strength this way, and that is increased cost due the increased alloying agent amounts and the strict manufacturing constraints.
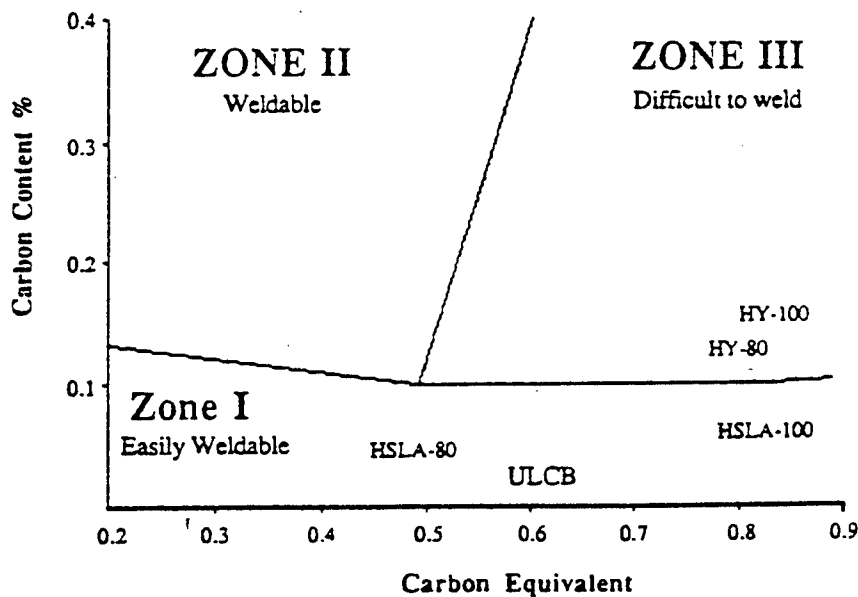
Figure 2.1   Graville diagram showing relative ease of weldability [Graville, 1978]

B.   CHARACTERISTICS OF ULTRA-LOW CARBON BAINITIC STEELS

Ultra-Low Carbon Bainitic (ULCB) steels are similar in composition to that of HSLA steels. Table 2.1 shows nominal compositions for ULCB-100 steel. ULCB takes the idea of substituting alloy strengtheners for carbon to a further extreme. Carbon content is cut in half again, and virtually all of the strengthening is achieved through the alloying agents. Higher amounts of molybdenum are generally substituted as Mo is very good strengthening agent, although in excess of 2 wt % it can have a negative affect on toughness [McDonald, 1992]. This alloy composition lends itself to

9

solid solution strengthening as in HSLA steel [Garcia, 1991].
Additionally, a fine bainite packet size and high dislocation
density due to a non-recrystallization controlled final roll
pass are effective strengtheners as in HSLA steels [Pickering,
1978].   Toughness is again achieved through the alloying
agents and through the basic bainitic microstructure of the
steel.   Garcia [1990] states that resistance to ductile
fracture is controlled chiefly by non-metallic inclusions, but
no other concurring opinions could be found. Figure 2.1 shows
how ULCB steel falls in the "easily weldable" region of the
Graville diagram which is the primary reason it is being
heavily studied for use in Naval construction both as base
plate, and in the case of this study, as a weld wire
consumable.

As the name implies, ULCB steels are primarily bainitic in
their as-rolled or as-welded microstructure. This is because
of their very low carbon content. With such low carbon there
is virtually no possibility of martensite formation. This
allows us to limit the quench and temper phase of
manufacturing, making initial production more cost effective.
The formation of bainite occurs when the steel cools from
austenite to its equilibrium state at room temperature
[Callister, 1991].   Bainite forms along with martensite,
ferrite, acicular ferrite, cementite, and pearlite, and is
sometimes difficult to distinguish from other microstructures
even for an observer with a highly trained eye. Bainite is

10

often characterized as either upper or lower bainite depending on its temperature of formation, and many materials scientists consider acicular ferrite to be a form of bainite [Yang, 1989].

Acicular ferrite is widely accepted as the most favorable microstructure for high toughness [Hart, 1987, Chen, 1988, and Francis, 1990]. It is nucleated intragranularly, and its fine, interwoven structure makes it difficult for cracks to propagate in a straight line leading to greater toughness in the metal. Acicular ferrite usually only occurs in weld metals with high oxygen contents, and the amount of this microstructure is largely dependent upon the particular welding process involved as far as heat input, oxygen content, alloy content, and prior austenite grain size are concerned [Grong, 1986, and Francis, 1990]. The right combination of the above can create favorable conditions for the formation of high concentrations of small non-metallic inclusions which serve as nucleation points for acicular ferrite.

C. GAS METAL ARC WELDING

Gas Metal Arc Welding (GMAW or MIG) is a welding process in which a consumable electrode is mechanically fed into the workpiece. The electrode and the work area itself are protected from the surrounding atmosphere by a cover gas. A typical MIG welding set up is shown in Figure 2.2. Typical gases in MIG welding are argon or some combination of CO_2 and

argon. Most of the MIG welds looked at in this study utilized C5 cover gas (5% CO_2, 95% argon).
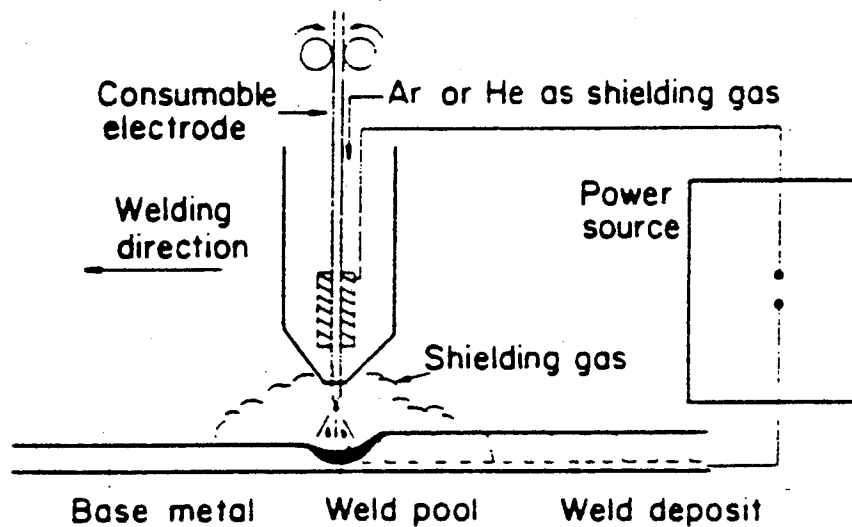

Figure 2.2 GMA welding process [Kou, 1987]

In any type of consumable electrode welding the electrode itself is the filler wire. In order to accomplish this the electrode must receive much more of the heat in order to melt for transfer to the workpiece and so direct current reverse polarity current is normally employed [Kou, 1987]. There are three basic methods of metal transfer to the weld: globular, spray and direct contact (short circuit). Globular transfer is generally preferred, but the actual method of transfer is

controlled by the power, electrode shape and size, and type of cover gas [Kou, 1987]. The high deposition rate of metal into the weld from MIG welding makes it highly desirable in situations where multi-pass welds are required. In comparison with TIG welding, MIG can accomplish the same deposition in approximately one third of the passes.

Some degree of reactive cover gas (such as 5% CO_2 in C5) is utilized to assist in arc stabilization. The addition of oxygen can result in a greatly increased number of non-metallic inclusions in the solidified weld as it combines with alloying elements such as aluminum, titanium and silicon. These alloying agents are referred to as deoxidizers as they tend to react with oxygen in the weld metal and form non-metallic inclusions which will be discussed in a later section. It is important to control the amount of oxygen in the weld, as too much will not only produce inclusions, but can lead to the formation of carbon monoxide which creates porosity in the solidified weld.

D. GAS TUNGSTEN ARC WELDING

Gas Tungsten Arc Welding (GTAW or TIG) is a welding process in which a non-consumable electrode is either used without a filler wire (autogeneously) or with an independently fed filler wire. The electrode and the work area are protected from the atmosphere by an inert shielding gas. Helium or argon are normally used, with argon being preferred

13

because it allows for a lower voltage drop across the arc and allows for easier arc initiation [Kou, 1987]. A typical TIG welding set up is shown in Figure 2.3.
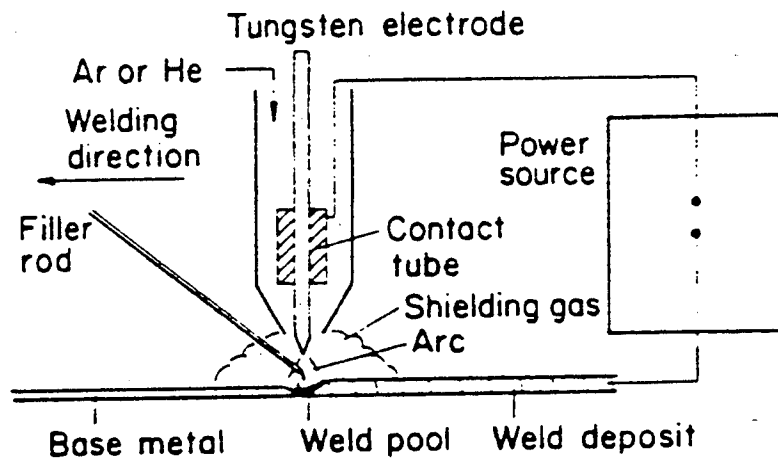
Figure 2.3 GTA welding process [Kou, 1987]

TIG welding is considered to be a very clean welding process because of its virtually complete shielding afforded from the use of an inert gas. The excellent shielding provides a very low tendency to form oxides or nitrides as both oxygen and nitrogen are virtually non-existent in TIG welds. Three basic modes of operation are commonly used in TIG welding, direct current straight, reverse and alternating polarity. As the TIG electrode is non consumable, when

14

reverse polarity is used and much of the power is directed to the electrode vice the workpiece, it is necessary to water cool the electrode.

One disadvantage of TIG welding versus MIG is the relatively low deposition rate. This means that several more passes must be made by skilled TIG welders or expensive equipment used in order to accomplish the same thing as a MIG weld. An increased number of passes does have the advantage though of having subsequent passes act as heat treatments allowing for grain refinement of previous passes.

E. COOLING RATE CONSIDERATIONS

Cooling rate considerations are of great importance to metallurgists involved with welding. During cooling from austenite many different microstructures can form, and often do so in varying degrees, to leave a final weld of multiple microstructures rather than one uniform microstructure. Martensite requires the quickest cooling rate as it is an athermal transformation. In order of slowing cooling rate martensite is followed by bainite (upper and lower), acicular ferrite, ferrite (side plate and Widmanstaten), and pearlite [Francis, 1990]. Acicular ferrite is the most desirable microstructure for reasons previously discussed, thus the cooling rate between 800 and 500 degrees Celsius is the important region to control. The actual time required in this particular temperature region to form a particular

15

microstructure varies from alloy to alloy according to the nature of the continuous cooling diagram and is controlled by manipulation of pre-heat, interpass temperatures, heat input and preheat. Figure 2.4 shows a continuous cooling diagram for HSLA-100. The desired cooling rate in this case would pass through the granular bainite region (GB) and form a small amount of martensite (M). The diagrams differ as alloy compositions vary, but this diagrams shows the general positions for all steels of this type.
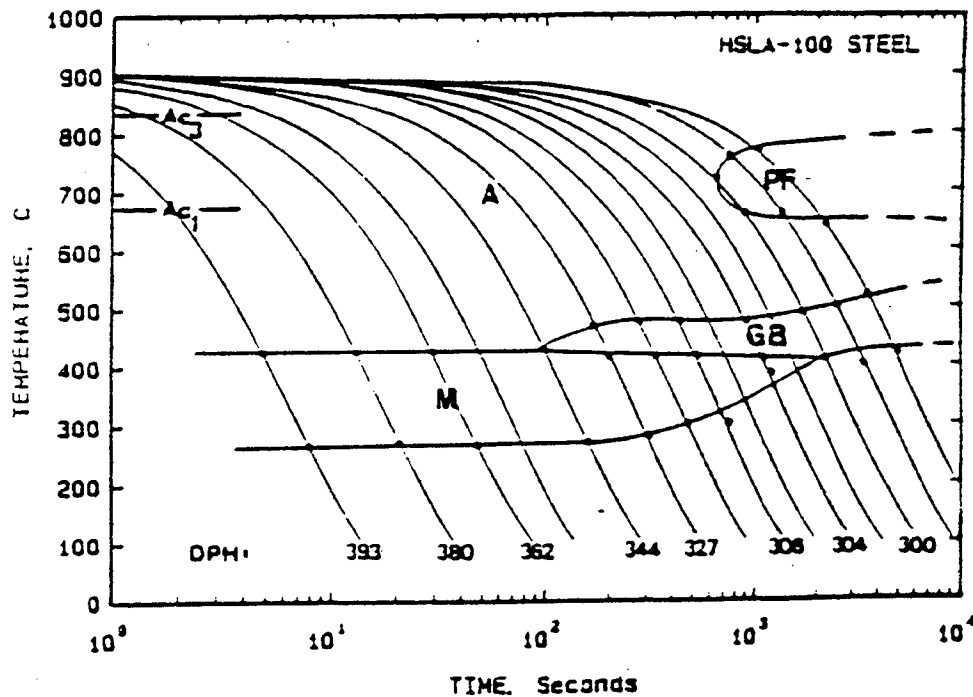
Figure 2.4 CCT diagram of HSLA-100 [Wilson, 1988]

F. NON-METALLIC INCLUSIONS

Non-metallic inclusions are commonplace in steels. Modern manufacturing techniques are fairly clean in both oxygen and sulfur, thus there are relatively few inclusions in as-manufactured steel. The average size of these inclusions is around three microns which can have a deleterious effect on toughness [Kiessling, 1978], but their number is small enough that they are not generally of concern. The non-metallic inclusions in welded sections of steels are of much greater interest.   Their size, frequency, composition, and distribution are primarily controlled by the type of welding process as it generally dictates oxygen content, heat inputs and cooling rates, and alloying elements in the weld metal itself [Francis, 1990]. The inclusions are formed as a result of alloying agents combining with oxygen to form non-metallic oxides.   Elements such as aluminum, titanium, silicon, chromium, and manganese are often referred to as deoxidizers as they readily combine with oxygen.

As oxygen is a key ingredient, we can surmise that in welding processes where there is little oxygen such as TIG, there will be few inclusions and they would be of the form resulting from the combination of oxygen with the more strongly deoxidizing elements such as aluminum and titanium.

Similarly, in welding processes with more oxygen there will be more inclusions and they can also include combinations with the less strongly deoxidizing elements such as manganese, silicon, or even chromium.

Inclusions are highly studied in steels because of their potential effect on the final microstructure and overall strength of the weld. Inclusions which are larger than two microns are known to be detrimental to strength and toughness, those which are smaller than two microns often serve to strengthen the weld [Kiessling, 1978]. As the small inclusions found in most high strength steel weldments are hard and non-deformable, they are effective in impeding dislocation movement and grain boundary growth which helps to strengthen the weld. Inclusions can also serve as nucleation sites for the formation of microstructures during the transition from austenite. Of particular interest to many researchers is the intragranular nucleation of acicular ferrite as it is believed by many to require titanium oxides (TiO and TiO_2), or other complex oxides which are at least titanium rich [Okihito, 1988].

1. Deoxidizers

Deoxidizers can broadly be described as any alloying element added to the weld through the weld wire consumable or fluxes for the purpose of combining with excess oxygen in the weld. Many of the alloying elements added to high strength

steels such as aluminum, silicon, titanium, manganese, and chromium are reactive in the presence of oxygen and combine to form complex oxides. The exact composition of the oxides is dependent upon many welding parameters, the primary factors of interest being alloy composition, oxygen content, and heat input.

Deoxidizers are important for two main reasons. First, they help to remove excess oxygen from the weld lessening the likelihood that carbon monoxide will form causing problems of weld porosity during solidification. Second, the non-metallic inclusions formed can be beneficial to weld strength if less than two microns in diameter and can serve as nucleation points for preferential microstructures such as acicular ferrite. In high strength steels many of the alloying agents are reactive with oxygen and thus must be supplemented in the weld to ensure that the proper composition is maintained even after we allow for some of the alloying agents to be "lost" in the formation of inclusions. This deficit is normally made up for by adding an excess of the more reactive elements such as aluminum and titanium to the weld through the weld wire consumable or a fluxing agent.

a. *Aluminum*

Aluminum is the strongest deoxidizing element commonly found in high strength steels. It forms Al_2O_3 which are fairly small in size [Kiessling, 1978]. As aluminum is

usually the strongest deoxident present in weld metal, we would expect to see the highest concentrations of Al_2O_3 in welds with low levels of oxygen where the aluminum will effectively "use up" most of the available oxygen.

b. **Silicon**

Silicon is a less strong deoxidizer than aluminum or titanium and typically forms SiO_2. It is normally maintained at levels less than 0.4% as to not be detrimental to fracture toughness [Abson, 1986]. Silicon is a solid solution strengthener and aids in increasing the fluidity of the weld pool assisting carbon monoxide and larger inclusions to work their way to the surface during weld solidification.

c. **Titanium**

Titanium is a relatively strong deoxidizer typically forming TiO_2 in high strength steel welds although some authors have suggested TiO is the deoxidation product. Again, since this is a strong deoxidizer it will form in higher proportion to weaker oxidizers when oxygen levels are low.

d. **Chromium**

Chromium is the weakest deoxidizer which will be discussed. Its oxide, Cr_2O_3, is not normally found in abundance because weld metal oxygen levels rarely reach a high enough level for there to be a sufficient amount to allow for the formation of Cr_2O_3 when strong deoxidizers such as

aluminum, titanium, or silicon are present. In order for Cr_2O_3 to form in high strength steels we would expect the oxygen levels to be so high that weld porosity from carbon monoxide formation to have become a problem.

      e.   Manganese

Manganese is a relatively weak deoxidizer which normally forms MnO. Although a weaker deoxidizer, it often shows up in large quantities of complex oxides. The large percentage of manganese usually present in weld metal allows it to take part in deoxidation despite being a weak deoxidizer. Manganese is also very important in removing sulfur from the weld. The formation of MnS vice FeS is very important as FeS is known to cause problems with solidification cracking [Kou, 1987]. The low surface tension of FeS combined with its low melting temperature allows it to form a thin coat of liquid on grains making them susceptible to cracking during solidification.

2.   Inclusion Composition in High Strength Steels

The total inclusion composition in weld metals is expected to be a combination of the oxides discussed: Al_2O_3, SiO_2, TiO_2, Cr_2O_3, and MnO. MnS is also expected to form as sulfur is removed from the weld by manganese. The final percentage of each of the oxides and sulfides will depend on the alloy composition of the weld metal, oxygen content, heat input and the welding process utilized [Francis, 1990]. As

21

previously discussed, the elements which are stronger deoxidizers will form in higher relative proportion in welds with lower levels of oxygen.

G. MACRO AND MICROSTRUCTURE OF GTAW AND GMAW WELD METALS

The macrostructure of MIG and TIG weld metals are distinctly different. TIG welds have relatively small, half spherical deposits. In a single pass, or the final pass of a multi pass weld, we expect a coarse macrostructure looking more columnar as the size of the deposit increases. MIG welds have much larger deposits which form in the shape of an upright horse shoe. This shape is often referred to as a papule. This elongated shape allows for solidification to begin at one region, normally the exterior, which is followed by a columnar-looking grain growth towards the center of the pool. The resulting columnar structure is likely to be susceptible to brittle fracture as the large grain boundaries can make for easy crack propagation.

ULCB steels are designed to be utilized with bainitic microstructure thus we expect a majority of the weld deposit to be either acicular ferrite or bainite. Improper cooling rate could lead to a less favorable microstructure such as martensite if cooled too fast, or ferrite if cooled too slow. A ferritic microstructure would have the advantage of being tougher than bainite because it is more ductile, but this increase in toughness would be at the expense of strength.

H. SCOPE OF PRESENT WORK

An ongoing effort has been underway between the Naval Surface Warfare Center (NSWC), Annapolis, and the Naval Postgraduate School (NPS) to determine optimum welding conditions for ULCB steels when used as weld wire consumables.

Previous work by Butler [1993] concluded that non-metallic inclusions had little effect on fracture toughness, but a continued effort is underway for a greater understanding of how the macro/microstructure and the presence/composition of non-metallic inclusions effects the overall strength and impact toughness of the weld deposit. NSWC has reported the standard TIG welds to be very tough in comparison to their MIG welds, yet lower in tensile strength than the MIG. The reason for this was explored as well as some non-traditional cover gas combinations on the two welding methods to determine if desirable characteristics of one weld could be transferred to another through a change in cover gas or heat input.

III. EXPERIMENTAL PROCEDURES AND RESULTS

Eight samples of HSLA-100 base plate were welded with UCLB-100 weld wire by NSWC. NSWC then performed tensile and impact toughness tests on the samples and forwarded them to NPS for optical and electron microscopy. The welding parameters for the samples are shown in Table 3.1.

TABLE 3.1 WELDING PARAMETERS STUDIED

(Nominal compositions shown in Table 2.1)

SAMPLE	WELD TYPE/ # OF PASSES	COVER GAS	HEAT INPUT (KJ/INCH)
CS2AT	TIG / 23	ARGON	60
CS2AM	MIG / 8	C5	60
MV1	MIG / 8	C5	60
MV2	TIG / 23	ARGON	60
MV3	TIG / 7	C5	78-161
MV4	MIG / 5	C5	97
MV5	MIG / 14	C5	30
MV6	MIG / 9	ARGON	60

These samples were analyzed optically for both macro and microstructure characteristics. A scanning electron microscope was used to catalog non-metallic inclusions for size, frequency, and volume fraction determinations. The transmission electron microscope was used for non-metallic

inclusion composition determination as well as for confirmation of the microstructure determined optically. Charpy V-notch samples were analyzed optically and in the SEM in order to determine the fracture mechanisms influencing sample resistance to brittle fracture.

A. SAMPLE PREPARATION

All eight samples received from NSWC were prepared in identical fashion for both optical and SEM analysis. The welds were cut in cross section, ground flat and then sanded progressively smoother with 240, 320, 400, and 600 grit silicon carbide paper. Final polishing was done using six, and then one micron diamond paste on selvyt polishing wheels. The samples were then ready for the SEM to conduct inclusion size and frequency data collection. After the SEM, the samples were etched in 5% nital for 20 seconds for optical microscopy.

In order to avoid interference problems from the steel matrix, chemical composition of the non-metallic inclusions was accomplished by removing the inclusions from the steel through a carbon extraction technique. To remove the inclusions, the sample was first deep etched in 5% nital for 60 seconds. This has the effect of "loosening" some of the inclusions from the steel. Next the etched samples were carbon coated using an Ernest Fullam MKII carbon coater to obtain a uniform carbon thickness over the weld of

approximately 250 angstroms (required from three to five strands depending on the position of the carbon fiber burn through). The carbon coated surface was scribed in small squares and returned to the 5% nital etchant to remove the carbon from the weld. When the carbon comes off the weld some of the inclusions of interest are captured in the carbon. The thin carbon sheets are floated off in methanol and placed in a 20% acetone, 80% water solution which unrolls the sheets because of the its high surface tension. The sections containing extracted inclusions were then floated on to a 400 mesh copper grid for EDX analysis in the TEM. A typical carbon extraction is shown in Figure 3.1, the inclusions are visible as small light colored spheres on the grid. The granular looking pattern is a replication of the etched weld deposit.
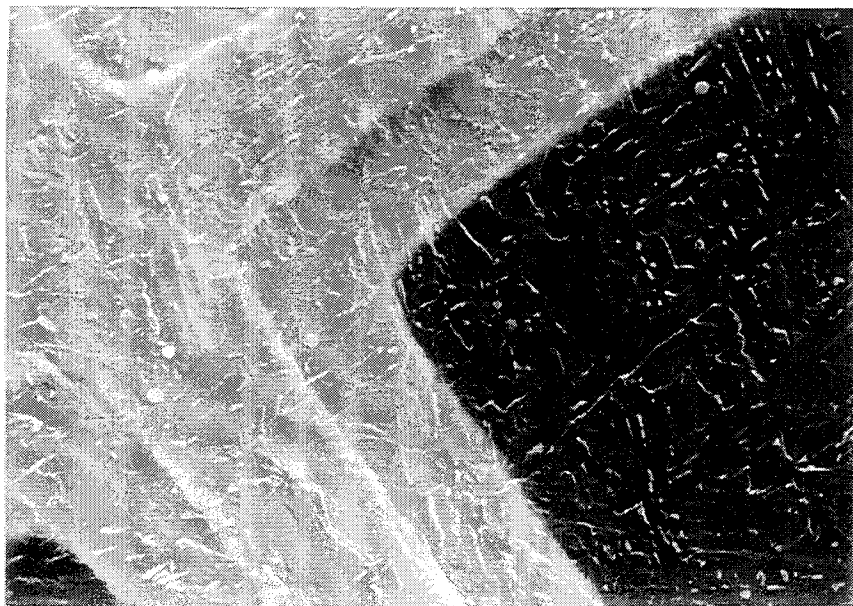
Figure 3.1 Typical carbon extraction on grid (2.13 kX)

The final sample preparation was to produce thin foil TEM samples of CS2AT and CS2AM for microstructural analysis. In order to accomplish this a 0.5 millimeter slice of the weld was taken using a low speed diamond saw. This sample was then thinned by hand to 150 microns (0.15 mm). The slice was etched to reveal the macrostructure of the weld so that three millimeter discs could be punched out for different regions of the weld (columnar, grain refined etc.). These discs were then thinned by hand using a Gatan 623 disc grinder to a thickness of 30-35 microns. Electropolishing was then conducted with a Struers Polipower electropolisher operating at 75 volts and 50 milliamps. A solution of 3% Perchloric acid, 35% 2-Butoxy Ethanol, and 62% Ethanol at -50 C was utilized to produce a hole and an adjacent thin region for microstructural analysis in the TEM.

B. OPTICAL MICROSCOPY

Macro and microstructure were analyzed using a Zeiss stereoscope for macro work and a Zeiss ICM 405 microscope for micro work. The macrostructure of the welds were as expected. Figure 3.2 shows a TIG weld (CS2AT) macrophotograph which was characteristic of the other TIG weldments (excepting MV3). TIG welds had relatively small depositions for each pass and showed primarily regions which had been grain refined by subsequent passes. The final pass in the TIG welds were

coarse and columnar in structure. Figure 3.3 shows a MIG weld (CS2AM) macrophotograph which was characteristic of the other MIG weldments. MIG welds had much larger depositions per pass and showed primarily regions of columnar grains in the papule. Very small regions of grain refinement were also present, again due to the heat from subsequent passes. Optical macrophotographs of the MV series weldments are shown in Appendix C.
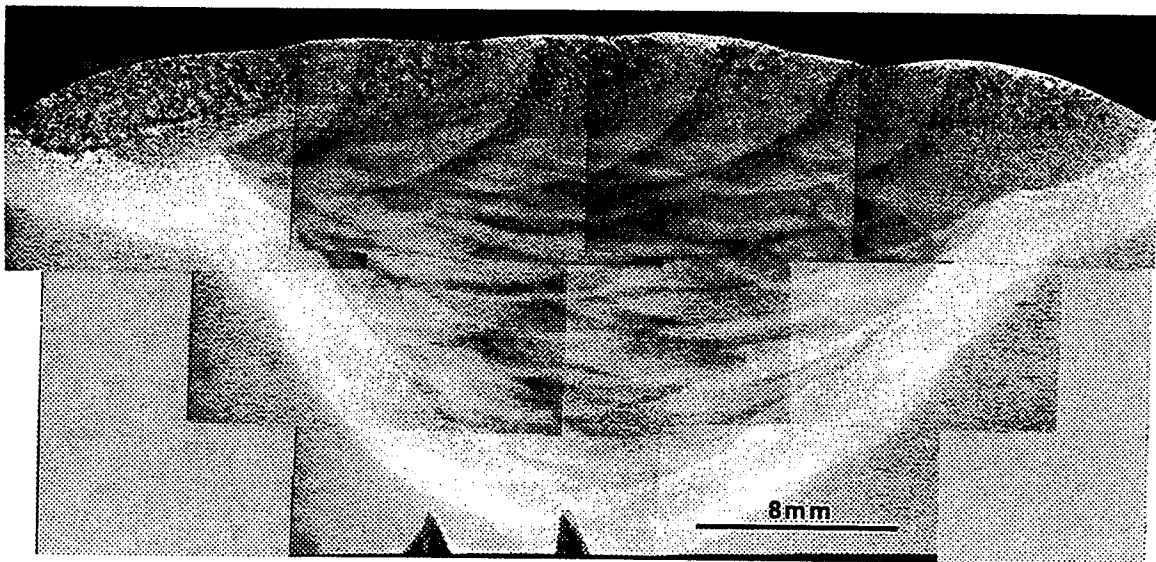
Figure 3.2 CS2AT Multi-run TIG weld
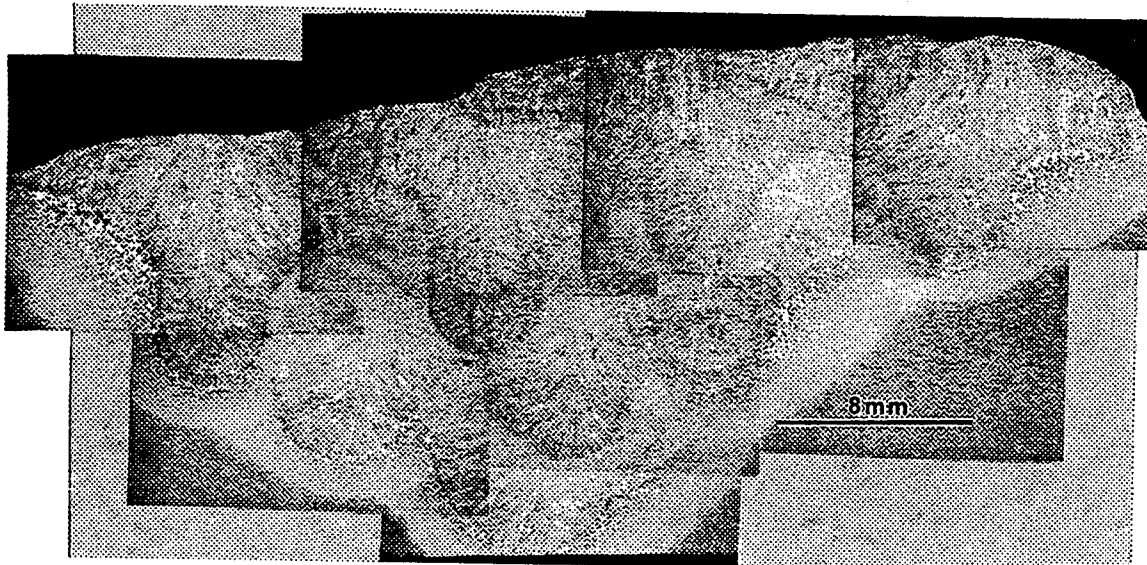
Figure 3.3   CS2AM   Multi-run MIG weld

Micrographs were taken of all samples to ascertain basic microstructural characteristics.   The expected bainite and/or ferrite microstructure was found in most instances, but not all.   The notable exception was that the grain refined regions of the TIG welds showed relatively equiaxed ferrite.   This is of added importance since almost all of the TIG welds are of a grain refined nature.   MV3 was extremely porous due to the excessive amount of oxygen introduced into the weld by using C5 cover gas in a TIG weld.   CS2AT and CS2AM were representative of the TIG and MIG welds and are shown in Figures 3.4 thru 3.7.
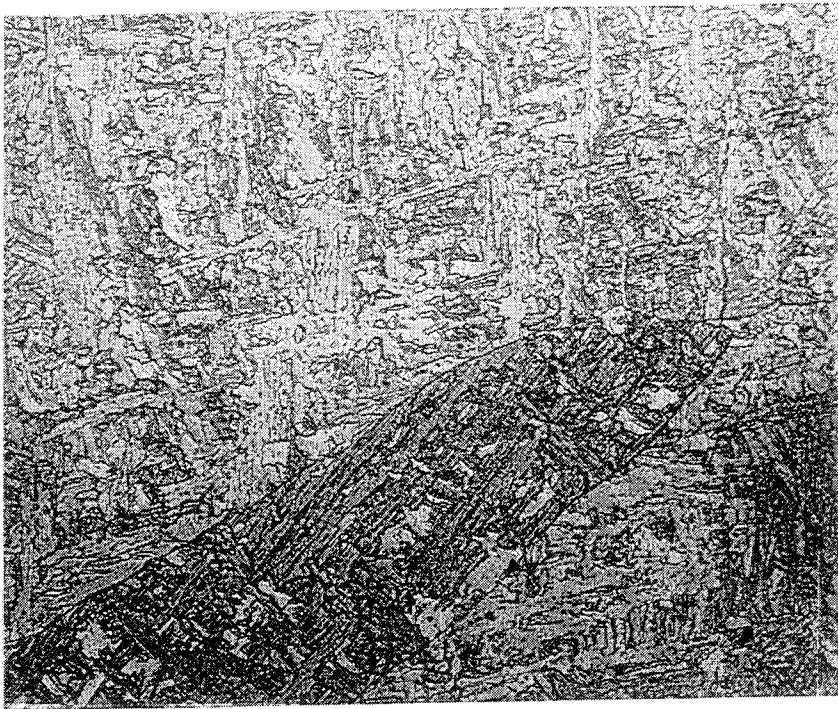
Figure 3.4 CS2AM Columnar Zone Side plate ferrite and
bainite (500 X)

Figure 3.5 CS2AM Recrystallized Zone Bainite (500 X)

Figure 3.6   CS2AT Final Pass   Bainite (500 X)
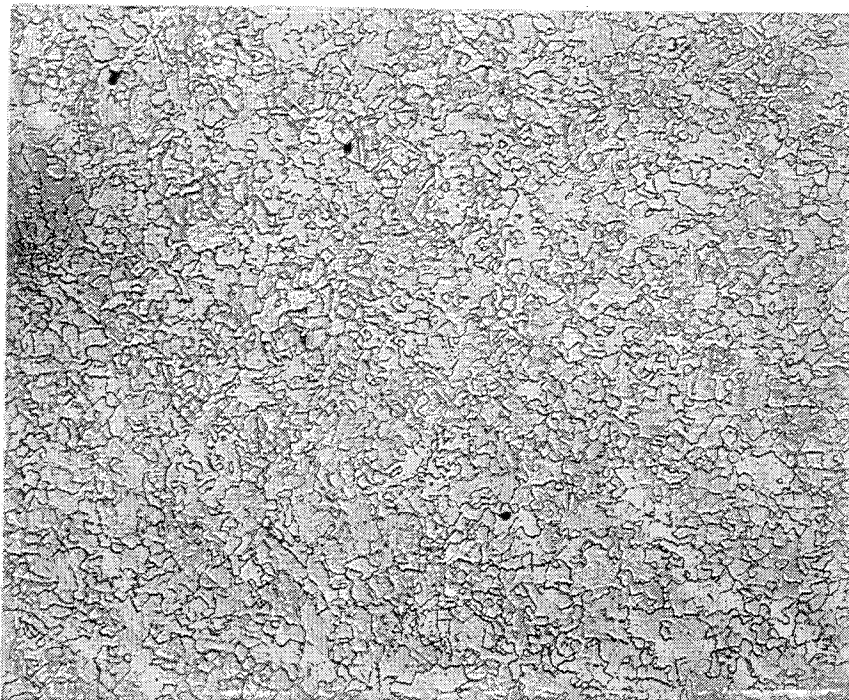
Figure 3.7   CS2AT Recrystallized Zone   Ferrite (500 X)

C.   SCANNING ELECTRON MICROSCOPY

All samples were analyzed using a Steroscan S200 scanning electron microscope (SEM) in the backscatter mode to determine size and frequency distributions of non-metallic inclusions. A LaB$_6$ filament energized to 20,000 volts was used to count 100 random fields for each sample at 7.04 kX magnification. The number, average size, standard deviation of size, and volume fraction was computed and is shown in Table 3.2. Graphical representations of inclusion size and frequency for each sample are shown in Appendix A.

TABLE 3.2   INCLUSION STATISTICS

	TOTAL NUMBER OF INCLUSIONS	AVERAGE SIZE (MICRONS)	SIZE STANDARD DEVIATION	VOLUME FRACTION (%)
CS2AT	307	0.317	0.099	0.135
CS2AM	291	0.563	0.294	0.403
MV1	271	0.524	0.258	0.325
MV2	209	0.332	0.127	0.101
MV3	214	0.613	0.352	0.351
MV4	259	0.574	0.263	0.372
MV5	364	0.439	0.199	0.306
MV6	366	0.385	0.153	0.237

D. TRANSMISSION ELECTRON MICROSCOPY

A JEOL JEM-100 CX II transmission electron microscope was used to determine inclusion composition of all samples. A LaB_6 filament was energized to 120,000 volts. Twenty extracted inclusions were analyzed for each sample using a Kevex model Delta windowless Energy Dispersive X-ray (EDX) spectrometer. The TEM was deemed to be the most appropriate device for EDX analysis of the inclusions as its software used for processing raw returns assumes that the sample is a thin foil. This is in contrast to the SEM which assumes that all samples are infinitely thick. The typical inclusion was less than one micron thick, thus the assumption of a thin foil is believed to be more correct in this application. The TEM EDX gave consistent data, a summary of which is shown in Table 3.3 with the raw data being shown in Appendix B.

The TEM was also used to corroborate the optically viewed microstructure determinations of CS2AT and CS2AM. TEM micrographs confirmed the optical micrographs showing there to be primarily bainite in the MIG weld and equiaxed ferrite in the grain refined zones of the TIG weld. Figures 3.8 thru 3.11 show representative TEM micrographs of CS2AT and CS2AM.

TABLE 3.3   SUMMARY OF INCLUSION COMPOSITION (Atomic/Oxide %)

	CS2AT	CS2AM	MV1	MV2	MV3	MV4	MV5	MV6
Al	69.52	2.52	4.27	25.33	28.52	3.87	0.99	44.26
Si	0.05	33.21	21.90	4.62	12.28	23.42	23.43	2.75
S	19.74	5.68	5.48	7.26	3.72	6.51	7.20	4.75
Ti	0.35	0.16	5.68	22.14	6.74	4.23	2.29	18.35
Cr	0.0	0.0	0.0	0.0	1.24	0.0	0.0	0.0
Mn	10.34	58.44	62.67	40.65	47.50	61.97	66.10	29.89
Al_2O_3	60.83	1.92	3.29	19.07	22.55	2.88	0.74	35.77
SiO_2	0.06	29.63	19.59	4.07	11.28	20.52	20.40	2.55
TiO_2	0.48	0.18	6.59	25.91	8.32	4.92	2.65	22.72
Cr_2O_3	0.0	0.0	0.0	0.0	1.47	0.0	0.0	0.0
MnO	0.0	54.81	57.61	33.93	47.26	56.50	59.61	27.20
MnS	38.62	13.46	12.92	17.02	9.13	15.18	16.61	11.76
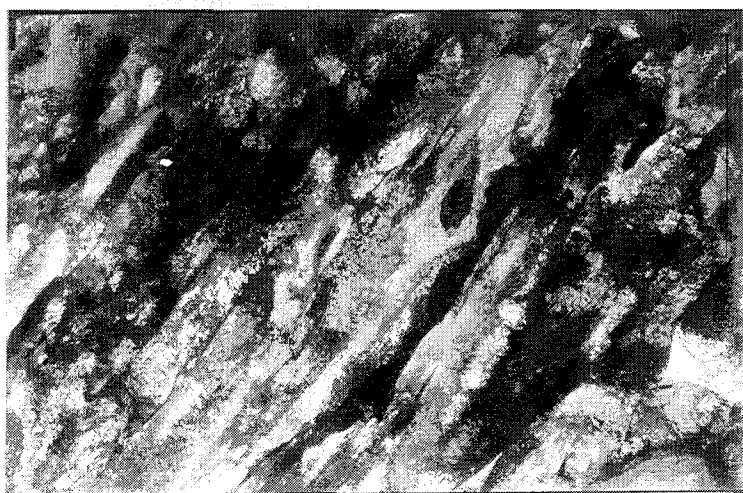
Figure 3.8   CS2AM Columnar Zone.   Bainite with
interlath retained austenite (7.2 kX)

34

Figure 3.9   CS2AM   Recrystallized Zone.   Granular
bainite with blocky and interlath
retained austenite. (10 kX)

Figure 3.10   CS2AT Final Pass.   Bainite with
interlath retained austenite. (10 kX)

Figure 3.11 CS2AT Grain refined zone ferrite (7.2 kX)

E. TENSILE STRENGTH AND FRACTURE TOUGHNESS

A determination of tensile strength and fracture toughness were conducted by NSWC Annapolis on samples CS2AT and CS2AM. Standard tensile samples and Charpy V Notch (CVN) samples were machined from the center of the weld pass. Three tensile samples were tested from each weld with the results shown in Table 3.4. The prepared Charpy samples were cooled to different temperatures prior to breaking. After the samples were broken, the fracture surfaces were judged for percentage of ductile fracture as ductile fracture is preferred to brittle fracture. CVN energy and percentage of ductile fracture results from NSWC Annapolis are shown in Figures 3.12 and 3.13.

36

TABLE 3.4   WELD TENSILE YIELD STRENGTH

CS2AT/CS2AM TENSILE YIELD STRENGTH (KSI)				
	SAMPLE 1	SAMPLE 2	SAMPLE 3	AVERAGE
CS2AT	85.8	83.4	100.6	89.9
CS2AM	101.5	104.3	101.0	102.3
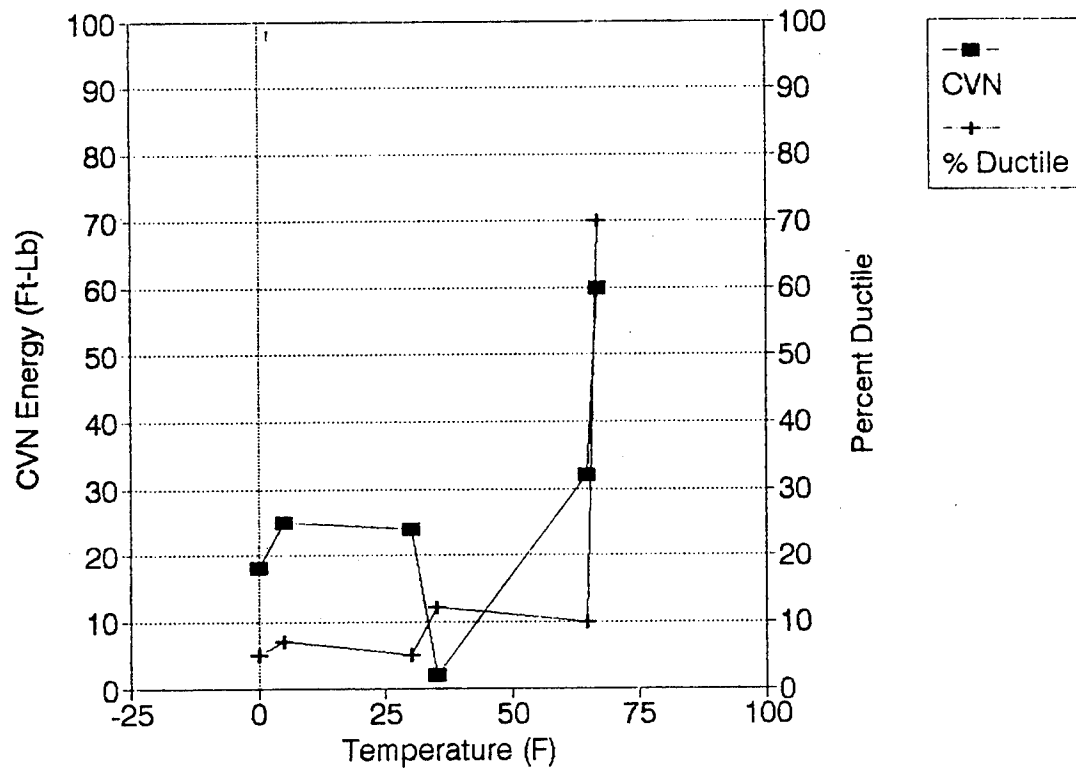
Figure 3.12   Charpy Impact   CS2AM
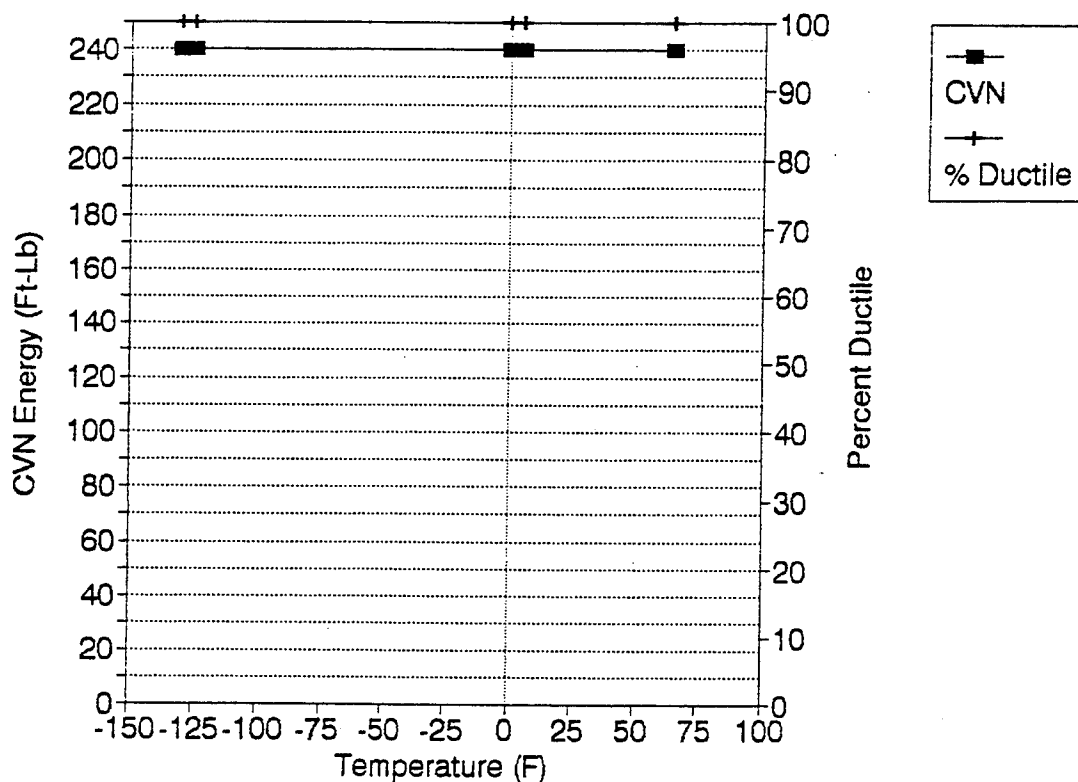
Figure 3.13 Charpy Impact CS2AT

The desired condition is to have high toughness with 100% ductile fracture, thus the results show TIG to have good toughness characteristics while MIG is poor. In an attempt to improve the impact characteristics of CS2AM and to see if the columnar macrostructure was responsible for the poor toughness, it was subjected to post weld heat treatments designed to simulate TIG weld passes. This was done by placing the CS2AM Charpy samples in a Gleeble machine to simulate the heating and cooling cycles of a 14 pass TIG weld of 60 KJ/inch (the same as CS2AT). Two slightly different Gleeble treatments were utilized, Heat Affected Zone One

38

(HAZ1) and HAZ2. HAZ1 was subject to temperatures of 1200, 1100, 1000, and 11 cycles at 914 degrees Celsius. HAZ2 started at 1300 and then was identical in progression to HAZ1 except that only 10 cycles at 914 degrees Celsius were performed. The results of CVN energy and percentage of ductile fracture for HAZ1 and HAZ2 are shown in Figures 3.14 and 3.15 and it can be seen that the effects of thermal cycling were to increase CVN toughness but to a level still significantly lower than the recrystallized TIG (Figure 3.13).
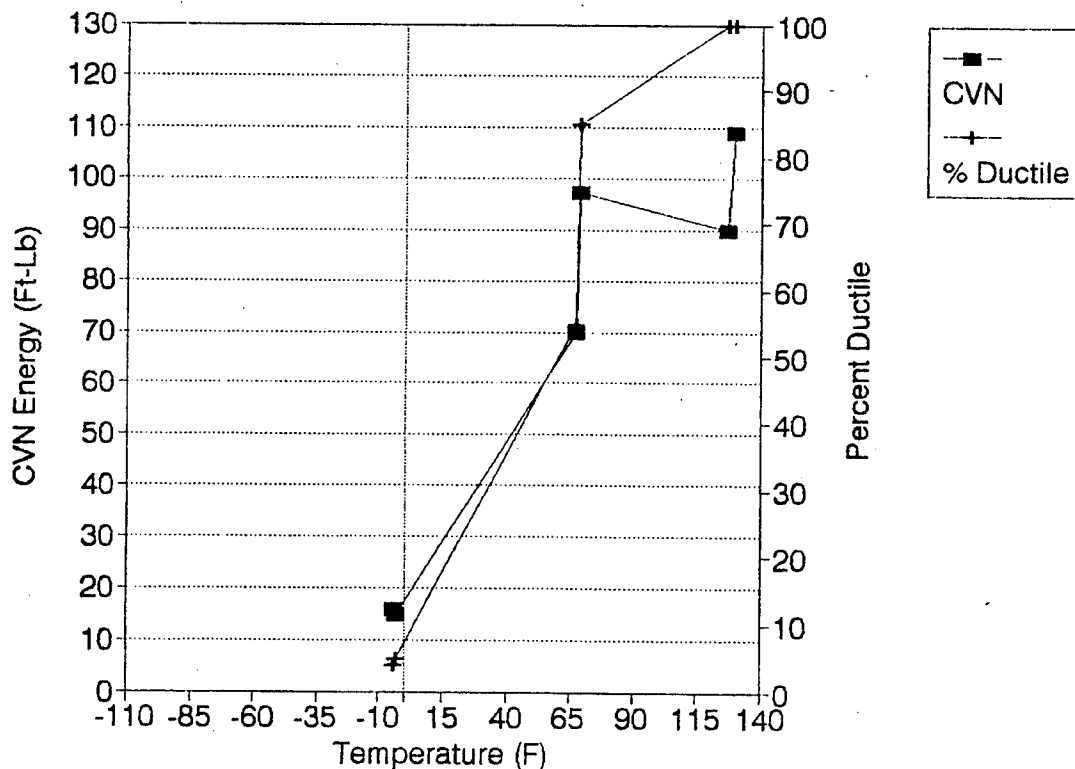
Figure 3.14   Charpy Impact   HAZ1
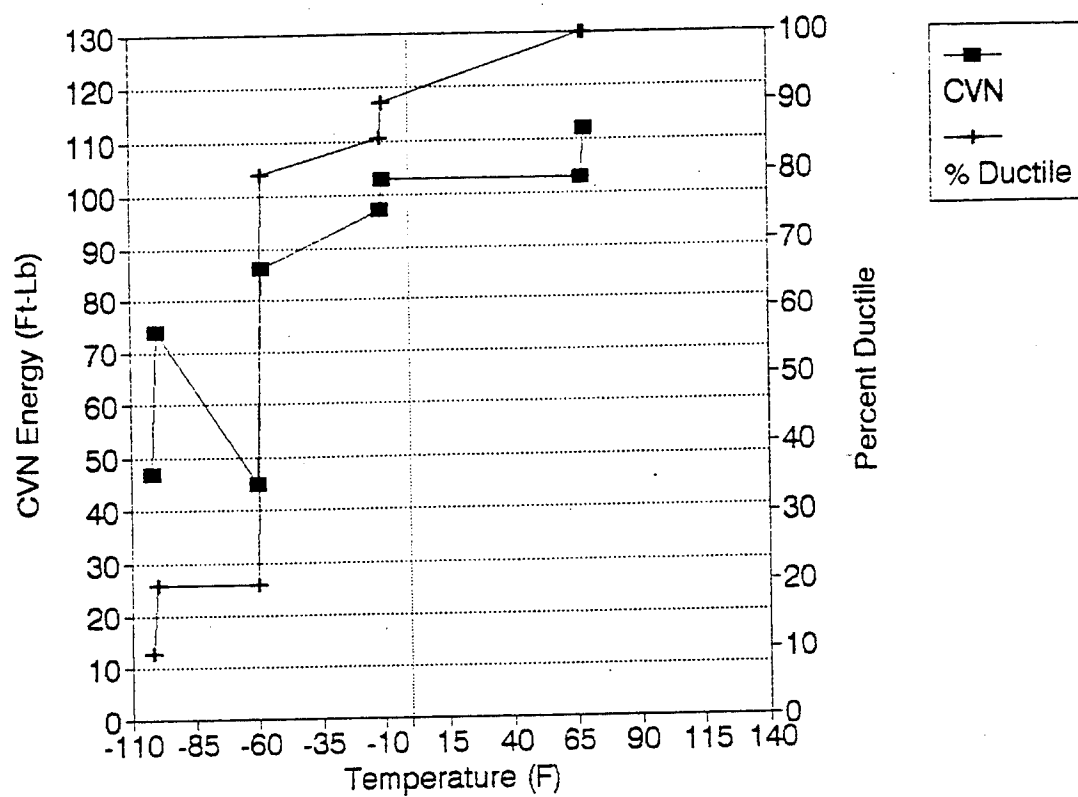
Figure 3.15   Charpy Impact   HAZ2

IV. ANALYSIS OF RESULTS

A. WELD THERMAL CYCLE

The desired microstructure for all weld metal samples supplied by NSWC Annapolis was 100% bainite since this would meet the 100 ksi strength requirements. As previously discussed, samples welded with MIG equipment achieved the desired microstructure although some side plate ferrite was present, while the TIG welds proved to be equiaxed ferritic over the entire recrystallized/grain refined zone. Since equiaxed ferrite usually requires slower cooling rates than bainite or acicular ferrite the time spent by the TIG welds in the important 800 to 500 degrees Celsius may have been excessive. Since the final pass of the welds are bainitic, the ferrite present is likely due to a cumulative effect of the multiple pass TIG weldment. Grain refined zones of the MIG welds also contained some ferrite, but large amounts of bainite were still present, and the overall amount of the recrystallized zone was much smaller.

B. WELD METAL COMPOSITION

Weld metal composition is important in terms of both filler metal alloy content and oxygen content. Exact levels of oxygen concentrations were not available for MV series

41

samples, but a complete analysis was conducted on CS2AT and CS2AM with results shown in Table 4.1.

TABLE 4.1 WELD METAL CHEMICAL COMPOSITION (wt %)

WELD METAL COMPOSITIONS AS DETERMINED BY LUVAK, INC.		
	CS2AT	CS2AM
Carbon	0.012	0.034
Manganese	1.05	1.29
Silicon	0.22	0.21
Phosphorus	0.005	0.005
Sulfur	0.004	0.011
Nickel	2.26	2.03
Molybdenum	0.97	0.89
Chromium	0.71	0.17
Niobium	0.046	0.027
Aluminum	0.021	0.018
Titanium	0.005	0.004
Copper	1.45	0.35
Oxygen	0.0010	0.0010
Nitrogen	0.0047	0.0045

The compositions listed in Table 4.1 were not exactly as expected. Specifically, the copper content in CS2AT was much higher than expected. This calls into question if the sample analyzed was cut exclusively from the weld pass. The higher

copper content of the HSLA base plate may be an answer if the sample strayed into it.

C. ANALYSIS OF NON-METALLIC INCLUSIONS

Hard, non-deformable non-metallic inclusions are important in composition, size and frequency to the overall strength and toughness of a metal as they serve as dislocation and grain boundary pinning sites, and often have a strong effect on microstructure during solidification. The composition of the inclusions in all welds analyzed were of a complex nature. Depending upon filler metal alloy content and oxygen composition, there was a core oxide comprised of complex aluminum, silicon, titanium, manganese, and chromium, oxides surrounded by the later forming manganese sulfide. A direct comparison of CS2AM to MV1 and CS2AT to MV2 for the purpose of showing that the same welding parameter would always yield the same results could not be made due to the differences in alloy content of the filler wires used in the CS2 series and MV series. The titanium oxide level in the CS2 series weld was very low, less than 1%, and thus almost no acicular ferrite was seen in the weldments.

Size, frequency, and volume fraction of the inclusions was able to be generalized by welding process and cover gas. TIG welds with Argon cover gas had the smallest and most uniform distribution of inclusions which gave a very low volume fraction for these clean welds. MIG welds produced larger

inclusions, a greater spread in the frequency and distribution, and yielded the highest volume fractions. The two exceptions to these rules were samples MV3 and MV6. MV3 showed characteristics which were much like MIG welds owing to its use of C5 cover gas, and MV6 (MIG) inclusion data was much like that of TIG welds due to its use of argon. In all cases though, the inclusions are deemed to be too small and too few to have much effect on the ductile to brittle transition temperature, or in upper shelf energy [Butler, 1993].

D. TENSILE STRENGTH AND FRACTURE TOUGHNESS

Tensile tests on CS2AT and CS2AM were as expected based on microstructure determinations. CS2AT failed to meet the 100 ksi standard. The fact that chemical composition results suggest that the tensile sample from this weld may not have been taken completely from the deposit is not considered significant. The ferritic microstructure in CS2AT would have caused a tensile yield strength failure alone. CS2AM was much more consistent in the three samples, all of which met the 100 ksi threshold. This was not surprising owing to its relatively regular bainitic microstructure.

Fracture toughness results from CS2AT and CS2AM corresponded exactly to what should have been expected based on microstructural findings. CS2AT showed identical readings for toughness with 100% ductile fracture over all temperatures tested. This is what would be expected from an equiaxed

ferritic steel. CS2AM, which was determined to be primarily bainitic with the weld metal having a columnar structure, displayed very poor toughness from brittle fracture at temperatures below room temperature. A comparison of CS2AM broken Charpy samples was made with a known brittle fracture surface (1018 steel @ -57 F). Although definitely brittle, the CS2AM sample exhibited a different macroscopic and microscopic appearance.

Figure 4.1 shows a side by side comparison of 1018 steel and a CS2AM sample. While the 1018 exhibits a relatively uniform cleavage surface, CS2AM has larger more regularly oriented surfaces. Both samples were then looked at in the SEM to gain a better understanding of the fracture mechanisms in effect. Figures 4.2 thru 4.5 show a 1018 sample with a text book brittle cleavage surface and CS2AM with a much more irregular surface. CS2AM had regular cleavage areas, ductile areas, and many large cracks. The closeness of these features suggests that the steel is inherently ductile, but is initially being driven to brittle fracture by some other mechanism. This mechanism is believed to be the columnar grain macrostructure of CS2AM which serves as an easy initiation point and propagation path for cracks.

Figure 4.1   1018/CS2AM Charpy fracture comparison (6.4 X)
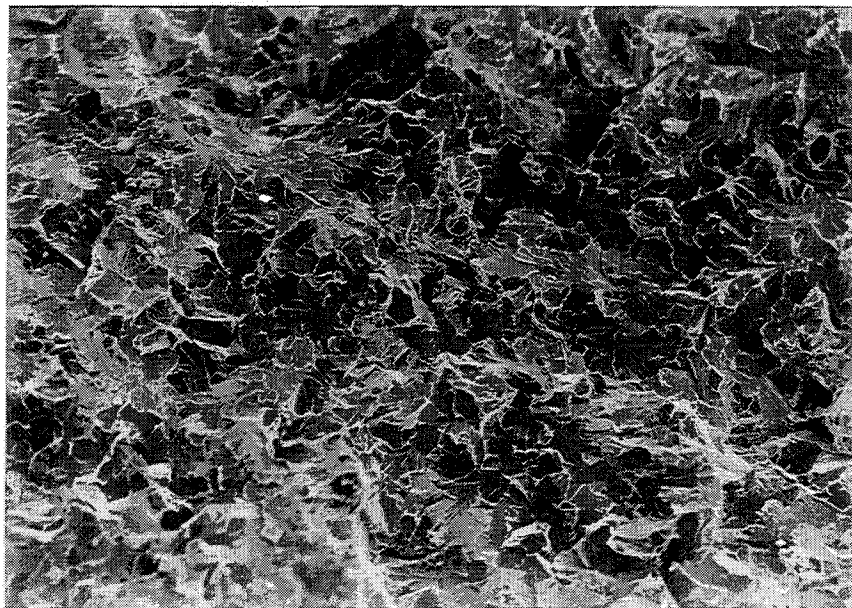
Figure 4.2   1018 steel brittle cleavage (169 X)

Figure 4.3 CS2AM Showing cracks in fracture surface
          possibly due to columnar grain structure
          (167 X)
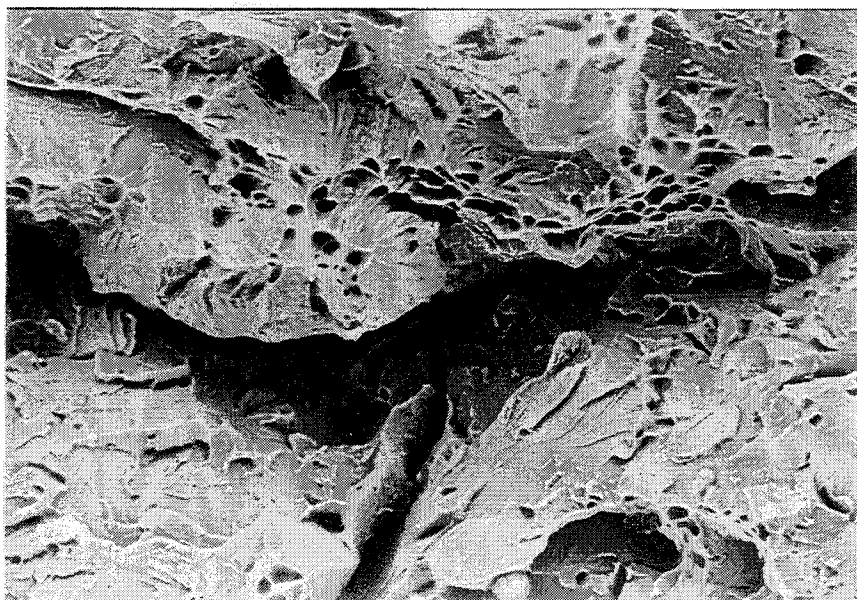
Figure 4.4 CS2AM As above at higher magnification (690 X)

HAZ1 and HAZ2 were experimental Gleeble treated samples which simulated TIG multipass heating and cooling cycles. Both heat treatments improved the ductile to brittle transition temperature by lowering it and improved CVN energy and the corresponding percentage of ductile fracture surface. HAZ2 was the most effective of the two, moving the transition temperature to -60 degrees Fahrenheit, and allowing the weldment to reach upper shelf CVN energy and to achieve nearly 100% ductile fracture over temperatures commonly experienced in Naval applications.

HAZ1 and HAZ2 were polished and etched for observation optically. This was done to ensure that the Charpy samples had been properly cut form the weld and to study the change in the microstructure. Figure 4.5 shows the "post Gleeble" microstructure of HAZ2. Note that the microstructure has become much more ferritic and equiaxed and looks very similar to the original CS2AT sample microstructure. Of particular note though was that even in HAZ2 the final CVN was less than half of that of CS2AT. The reason for this is not known, and could have something to do with how the grains reformed during the Gleeble treatment. A measurement of grain size in CS2AT grain refined zone done on optical micrographs showed a grain size of 4.7 microns, approximately six times larger than the grain size shown in TEM micrographs. This means that there is a substructure within the CS2AT ferrite grains. This could be considered to be somewhat like bainite where one observes

"packets" with a size similar to the prior austenite grain size with a lath structure enclosed inside the packets which is only positively revealed by TEM. Why the substructure of the TIG recrystallized grains is equiaxed is a mystery, but during the Gleeble cycles Mo_2C and/or NbCN could be precipitated leading to a very fine austenite grain size which did not allow the extensive growth of bainite laths with a high dislocation density. The hardenability of this steel would seem too high to allow the formation of proeutectoid ferrite. Further TEM work is necessary if this microstructure is to be understood. It is unknown if there is a similar substructure in the microstructure of HAZ1 or HAZ2. This could be an explanation of why HAZ2 did not achieve the same level of toughness as CS2AT if it did not grow the same subgrains during the Gleeble treatment. A TEM examination of the HAZ2 microstructure is necessary to resolve this issue.

An additional possible deleterious effect on toughness is due to the presence of inclusions greater than one micron. In general the effect of inclusions was not deemed significant, as they were mostly very small, but they cannot be totally ruled out as a possible contributing factor.
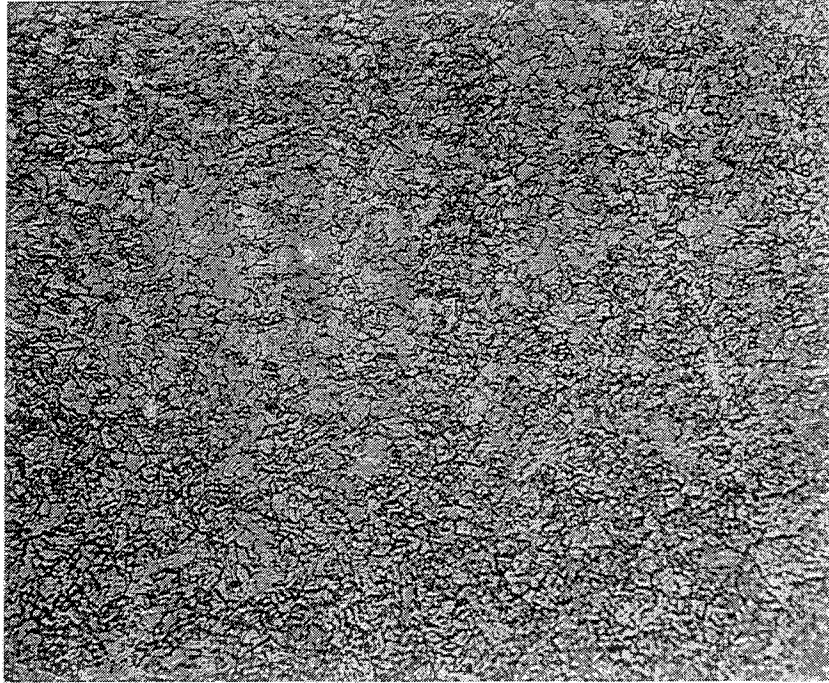
Figure 4.5   HAZ2 ferrite (500 X)

V. SUMMARY

A. CONCLUSIONS

1. Strength and Fracture Toughness

Strength and fracture toughness of ULCB-100 weld wire consumables is very controllable through manipulation of welding parameters. Weld metal microstructure is critical to tensile strength. Failure to achieve lath bainite leaves ULCB-100 short of the desired tensile yield strength. The overall macrostructure of the weld appears dominant in fracture toughness, but the presence of inclusions over one micron should not be totally overlooked. Some means of correcting for the columnar grain macrostructure must be devised if toughnesses are to be improved.

2. Inclusion Composition

Inclusion composition and frequency in ULCB-100 steel can be controlled through manipulation of weld wire alloy and oxygen content and the welding process employed. The use of carbon extraction for removal of inclusions prior to composition analysis lead to much more consistent and repeatable data due to less interference from the steel matrix. The thin foil assumption of the software in the EDX

used for TEM analysis combined with the better resolution of the TEM makes it the best choice for inclusion composition analysis.

B. RECOMMENDATIONS FOR FUTURE STUDY

There is much room for continued study in the realm of ULCB-100 weld wire consumables for Naval applications. Specifically I recommend:

●MIG and TIG weldments of nearly identical microstructures be compared for strength and toughness determinations to add the last piece of evidence necessary to be certain of the detrimental effect of columnar grains on toughness.

●Weld passes of identical heat input and welding type be used with differing oxygen content cover gases in order to produce differing inclusion compositions in the same macro/microstructure. This will allow for a more direct determination of the effect of differing inclusion size, frequency and compositions on final weld strength and toughness.

●The use of the carbon extraction technique and the thin foil EDX assumption for TEM analysis of inclusion composition should be utilized in all future study where inclusion composition is important.

●A tensile test should be conducted on HAZ1 and HAZ2 samples to see if how much of the CS2AM strength is retained. The microstructure of HAZ1 and HAZ2 should be analyzed in the TEM to check for the presence of substructures which may not be visible optically.

APPENDIX A   INCLUSION SIZE VS. FREQUENCY
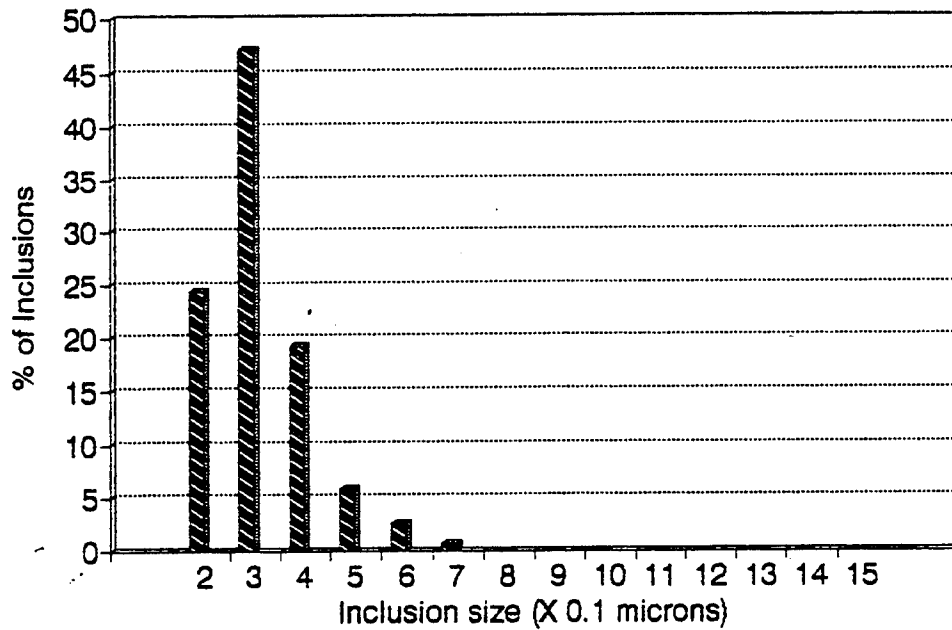
Figure A.1   CS2AT
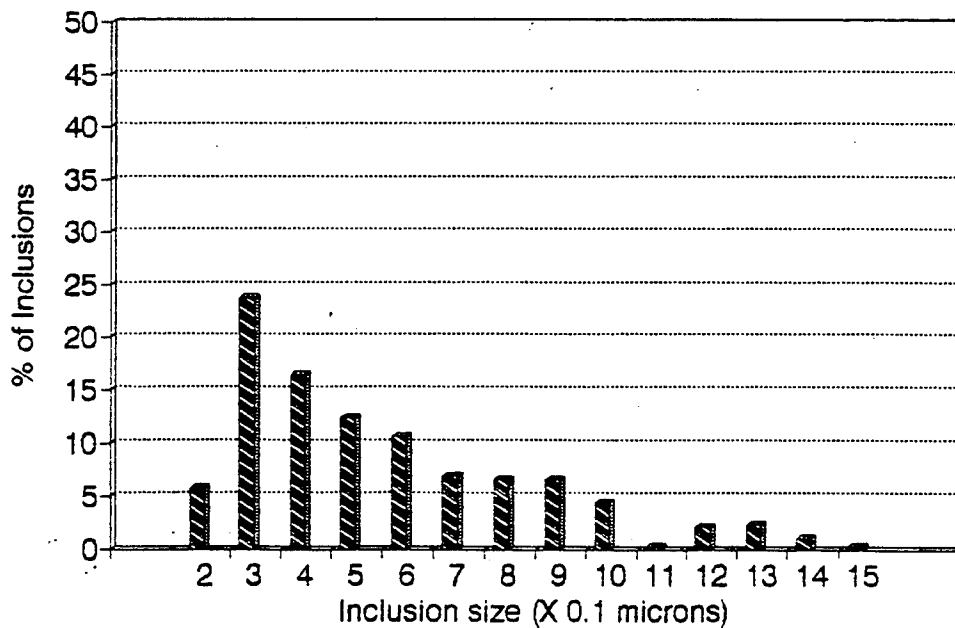
Figure A.2   CS2AM
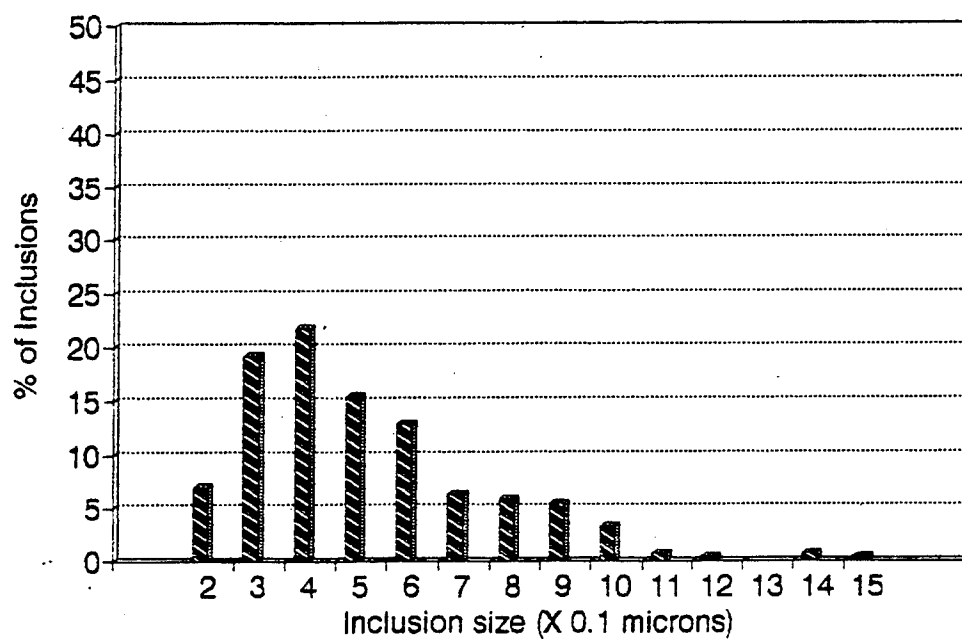
Figure A.3   MV1
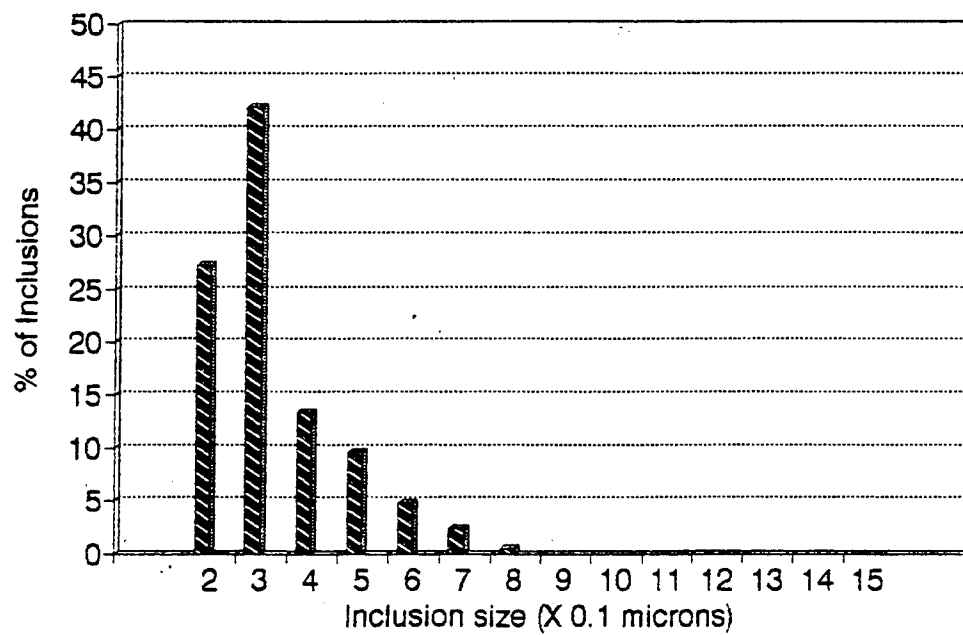
Figure A.4   MV2
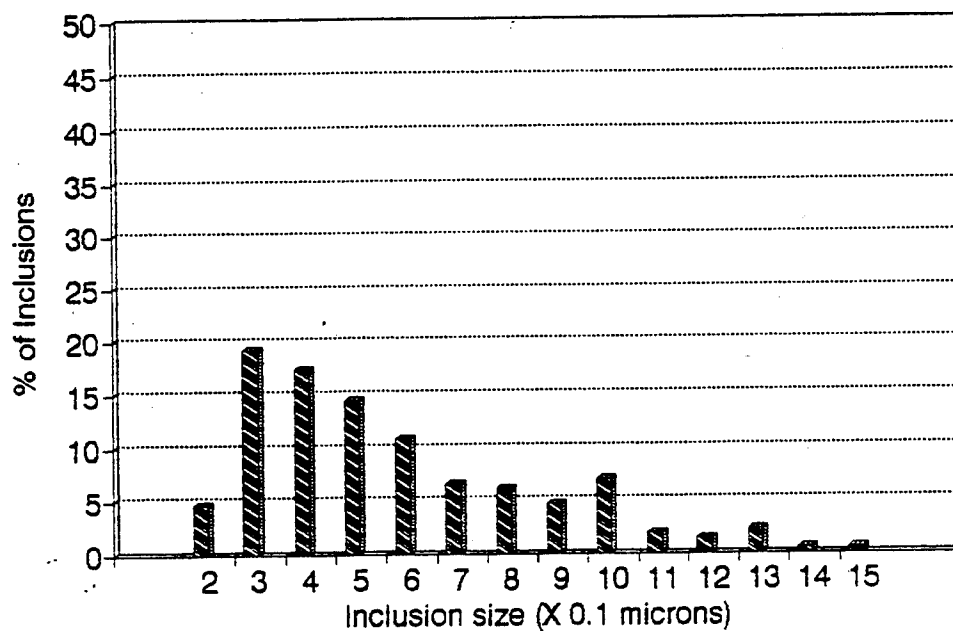
Figure A.5   MV3
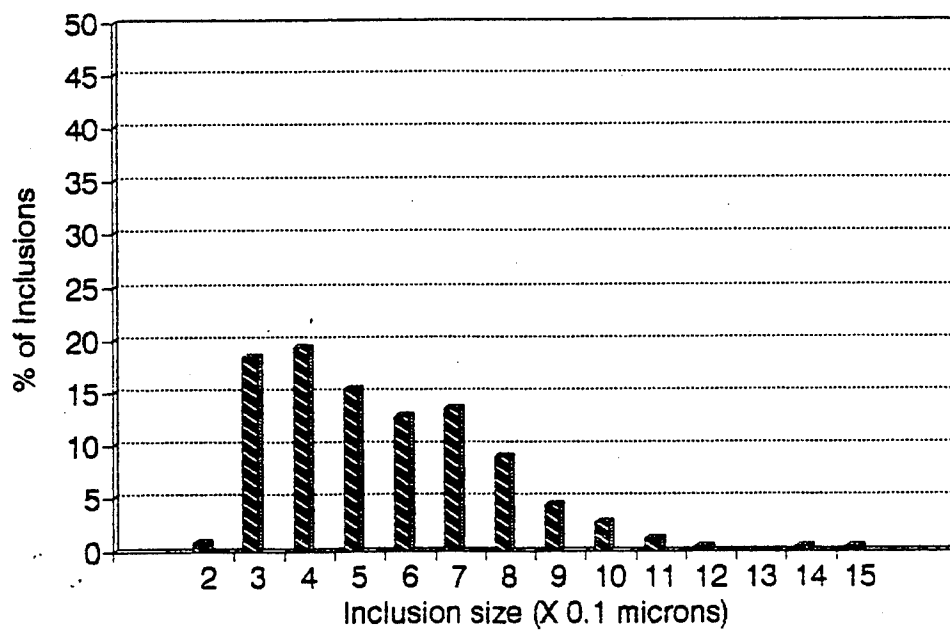
Figure A.6   MV4
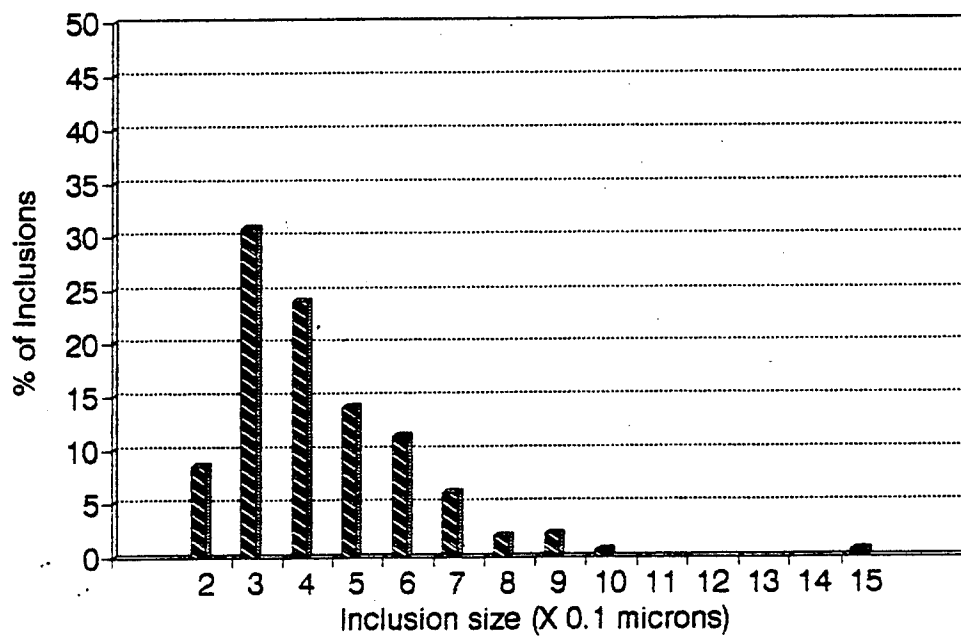
Figure A.7   MV5
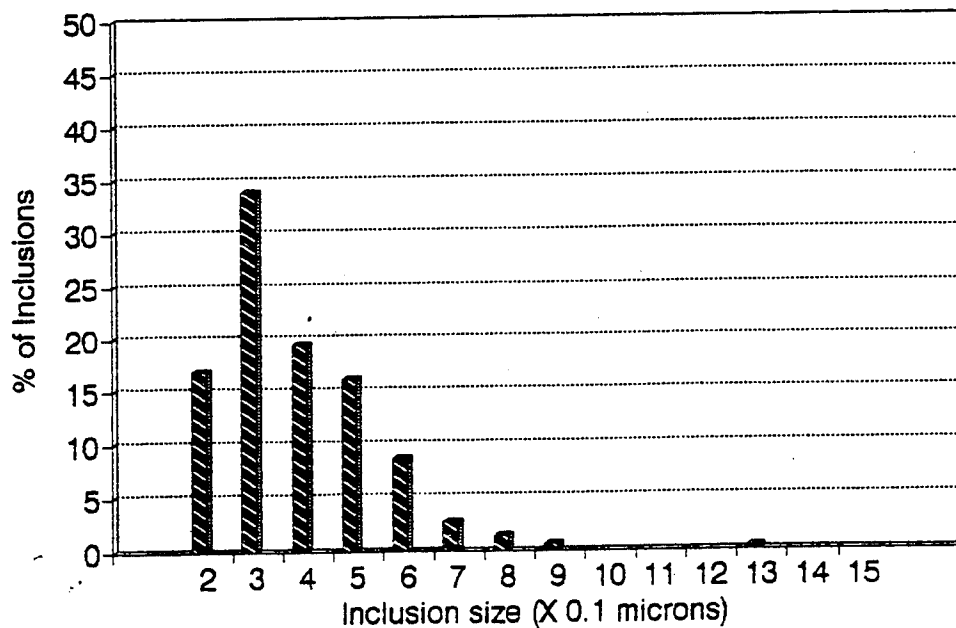
Figure A.8   MV6

APPENDIX B INCLUSION COMPOSITION

TABLE B.1 CS2AT CHEMICAL INCLUSION COMPOSITION

CS2AT: GTAW 60 KJ/IN ARGON COVER					
ATOMIC %					
	Al	Si	S	Ti	Cr	Mn
1	84.33	0.39	11.11	0.59	0.0	3.57
2	59.88	0.0	26.37	0.0	0.0	13.76
3	59.28	0.0	26.88	0.0	0.0	13.84
4	59.81	0.0	19.95	0.0	0.0	20.20
5	66.72	0.0	23.42	0.0	0.0	10.36
6	72.18	0.0	20.41	0.0	0.0	7.41
7	80.15	0.0	12.81	0.0	0.0	7.04
8	66.62	0.0	23.39	0.0	0.0	9.99
9	65.91	0.0	22.12	1.18	0.0	10.80
10	97.75	0.0	2.25	0.0	0.0	0.00
11	67.11	0.0	26.42	0.0	0.0	6.47
12	79.18	0.0	13.23	0.0	0.0	7.59
13	83.51	0.0	9.41	0.63	0.0	6.45
14	54.69	0.30	28.47	0.50	0.0	16.20
15	61.53	0.0	27.62	0.0	0.0	10.86
16	68.21	0.0	20.05	0.65	0.0	11.09
17	67.59	0.0	17.59	0.0	0.0	14.82
18	78.90	0.0	8.57	3.15	0.0	9.38
19	66.64	0.0	25.89	0.39	0.0	7.08
20	51.10	0.36	28.76	0.0	0.0	19.78
AVE	69.52	0.05	19.74	0.35	0.0	10.34
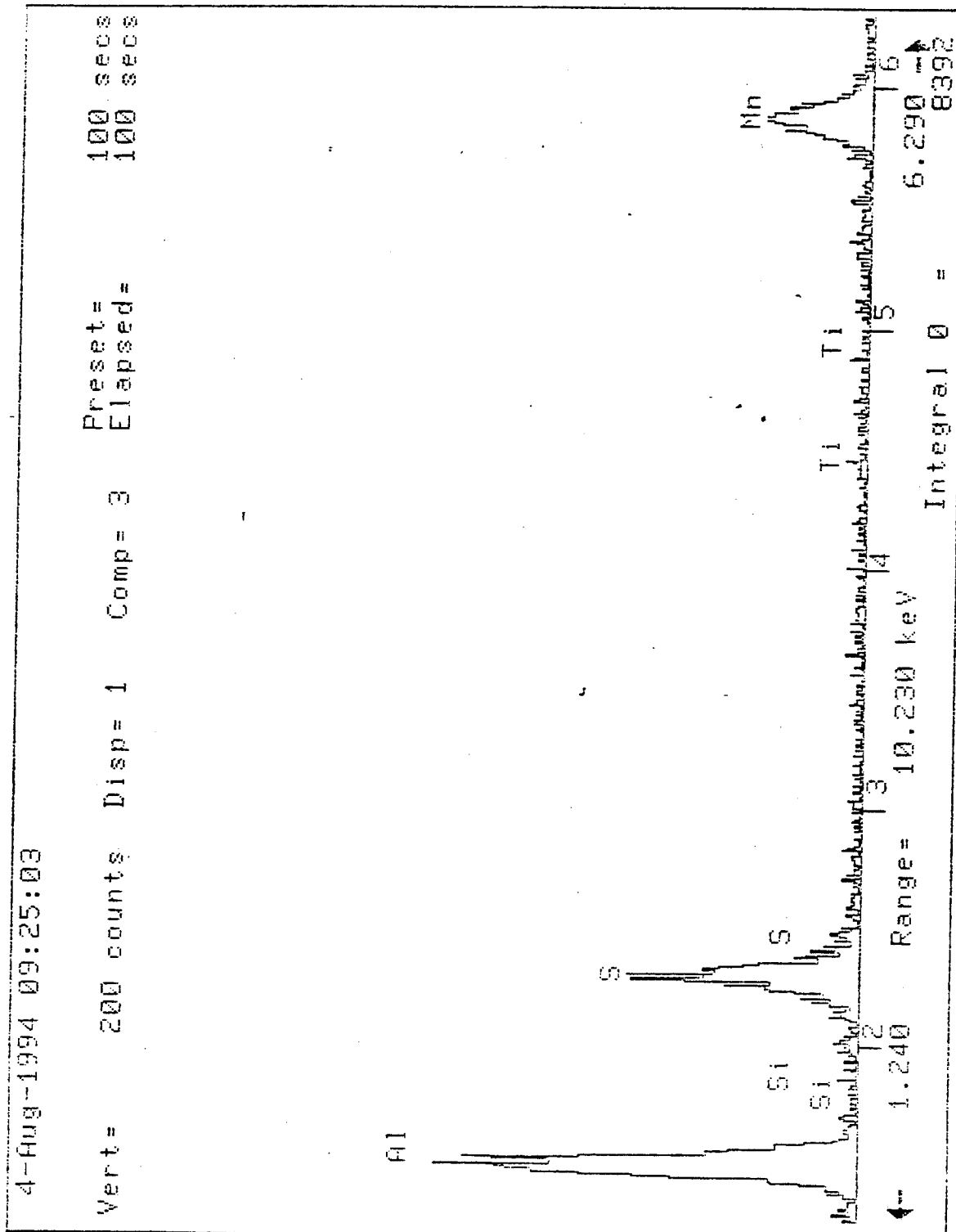
Figure B.01   Typical EDX   CS2AT

TABLE B.2   CS2AT CHEMICAL OXIDE INCLUSION COMPOSITION

CS2AT: GTAW 60 KJ/IN ARGON COVER					
OXIDE/SULFIDE %					
	Al_2O_3	SiO_2	TiO_2	Cr_2O_3	MnO	MnS
1	77.98	0.49	0.86	0.0	0.0	50.28
2	49.72	0.0	0.0	0.0	0.0	50.28
3	49.09	0.0	0.0	0.0	0.0	50.91
4	50.13	0.0	0.0	0.0	0.0	49.87
5	56.40	0.0	0.0	0.0	0.0	43.60
6	63.01	0.0	0.0	0.0	0.0	36.99
7	72.82	0.0	0.0	0.0	0.0	27.18
8	56.82	0.0	0.0	0.0	0.0	43.18
9	56.09	0.0	1.57	0.0	0.0	42.34
10	96.51	0.0	0.0	0.0	0.0	3.49
11	57.07	0.0	0.0	0.0	0.0	42.39
12	71.65	0.0	0.0	0.0	0.0	28.35
13	77.15	0.0	0.91	0.0	0.0	21.95
14	44.52	0.29	0.44	0.0	0.0	54.75
15	51.27	0.0	0.0	0.0	0.0	48.73
16	58.73	0.0	0.87	0.0	0.0	40.40
17	58.35	0.0	0.0	0.0	0.0	41.65
18	71.50	0.0	4.47	0.0	0.0	24.02
19	56.59	0.0	0.51	0.0	0.0	42.90
20	41.14	0.34	0.0	0.0	0.0	58.52
AVE	60.83	0.06	0.48	0.0	0.0	38.62

TABLE B.3   CS2AM CHEMICAL INCLUSION COMPOSITION

CS2AM: GMAW 60 KJ/IN C5 COVER					
ATOMIC %					
	Al	Si	S	Ti	Cr	Mn
1	0.36	31.62	13.75	0.0	0.0	54.27
2	0.0	38.02	5.12	0.19	0.0	56.67
3	0.87	34.01	6.83	0.0	0.0	58.29
4	1.10	32.72	4.93	0.0	0.0	61.25
5	2.22	30.70	5.36	0.28	0.0	61.44
6	3.40	29.46	3.51	0.34	0.0	63.29
7	2.71	30.92	4.16	0.18	0.0	62.03
8	4.64	33.03	2.26	0.17	0.0	59.90
9	4.05	32.35	3.88	0.07	0.0	59.64
10	1.76	36.42	10.00	0.0	0.0	51.82
11	3.59	29.41	6.08	0.57	0.0	60.36
12	1.49	36.77	6.80	0.0	0.0	54.94
13	1.54	32.64	6.46	0.14	0.0	59.22
14	0.95	32.67	5.83	0.13	0.0	60.43
15	2.77	32.18	4.65	0.30	0.0	60.10
16	0.54	34.28	9.61	0.0	0.0	55.57
17	4.60	35.01	2.41	0.46	0.0	57.52
18	4.21	38.83	3.23	0.0	0.0	53.73
19	5.62	34.03	3.40	0.0	0.0	56.95
20	3.99	29.10	5.33	0.27	0.0	61.30
AVE	2.52	33.21	5.68	0.16	0.0	58.44
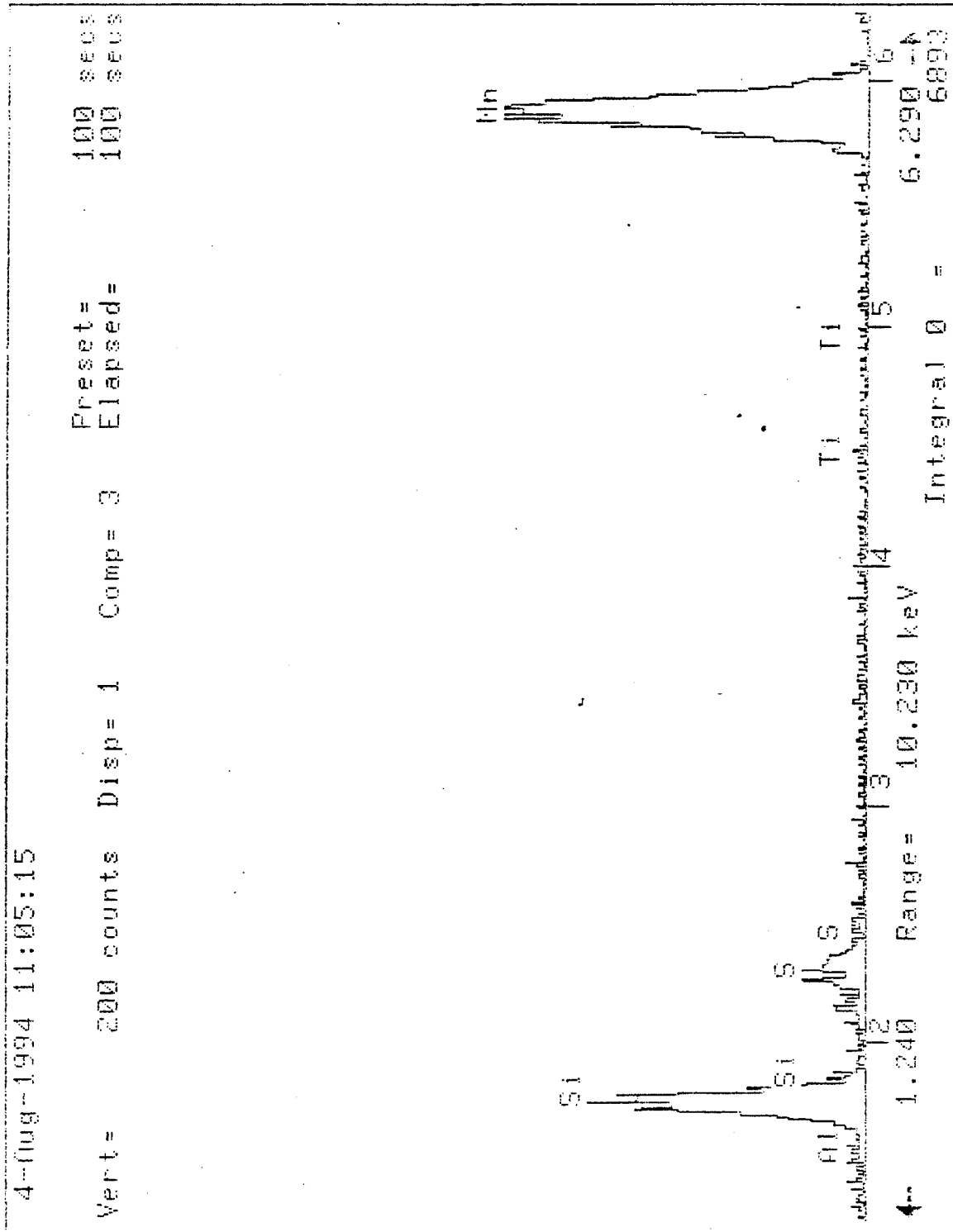
Figure B.02   Typical EDX   CS2AM

TABLE B.4 CS2AM CHEMICAL OXIDE INCLUSION COMPOSITION

CS2AM: GMAW 60 KJ/IN C5 COVER					
OXIDE/SULFIDE %					
	Al_2O_3	SiO_2	TiO_2	Cr_2O_3	MnO	MnS
1	0.27	27.66	0.0	0.0	40.03	32.04
2	0.0	33.95	0.22	0.0	53.65	12.18
3	0.66	30.18	0.0	0.0	53.00	16.16
4	0.83	29.07	0.0	0.0	58.42	11.68
5	1.68	27.26	0.33	0.0	58.06	12.68
6	2.57	26.25	0.41	0.0	62.43	8.34
7	2.05	27.55	0.21	0.0	60.31	9.88
8	3.55	29.78	0.21	0.0	61.03	5.44
9	3.08	29.02	0.09	0.0	58.53	9.28
10	1.33	32.40	0.0	0.0	42.57	23.70
11	2.70	26.12	0.67	0.0	56.11	14.40
12	1.13	32.84	0.0	0.0	49.85	16.18
13	1.16	28.98	0.16	0.0	54.42	15.28
14	0.71	28.97	0.15	0.0	56.38	13.78
15	2.10	28.72	0.35	0.0	57.79	11.04
16	0.40	30.29	0.0	0.0	46.66	22.64
17	3.53	31.64	0.56	0.0	58.48	5.80
18	3.24	35.25	0.0	0.0	53.68	7.82
19	4.31	30.78	0.0	0.0	56.71	8.20
20	3.01	25.91	0.32	0.0	58.11	12.64
AVE	1.92	29.63	0.18	0.0	54.81	13.46

TABLE B.5   MV1 CHEMICAL INCLUSION COMPOSITION

MV1:	GMAW	60 KJ/IN		C5 COVER	
ATOMIC %					
	Al	Si	S	Ti	Cr	Mn
1	2.73	19.24	4.77	10.10	0.0	63.16
2	1.13	24.20	3.15	2.43	0.0	69.10
3	2.13	20.18	15.48	1.89	0.0	60.33
4	0.57	29.64	1.19	1.53	0.0	67.07
5	3.32	21.30	4.08	2.95	0.0	68.34
6	3.45	20.66	5.92	2.77	0.0	67.20
7	2.64	22.56	3.88	9.50	0.0	61.42
8	6.01	23.14	2.41	7.03	0.0	61.42
9	4.91	21.12	4.94	6.51	0.0	62.51
10	3.47	21.88	3.10	8.70	0.0	62.84
11	6.23	23.51	3.21	5.39	0.0	61.66
12	4.66	19.12	9.66	3.83	0.0	62.73
13	4.57	14.04	3.77	3.61	0.0	74.01
14	6.41	25.80	9.65	1.51	0.0	56.63
15	4.98	21.74	7.50	7.05	0.0	58.73
16	0.92	24.97	4.66	2.51	0.0	66.93
17	6.98	24.87	7.60	4.51	0.0	56.04
18	5.21	21.85	3.70	8.82	0.0	60.42
19	8.33	15.13	6.54	16.84	0.0	53.16
20	6.74	22.97	4.20	6.32	0.0	59.76
AVE	4.27	21.90	5.48	5.68	0.0	62.67
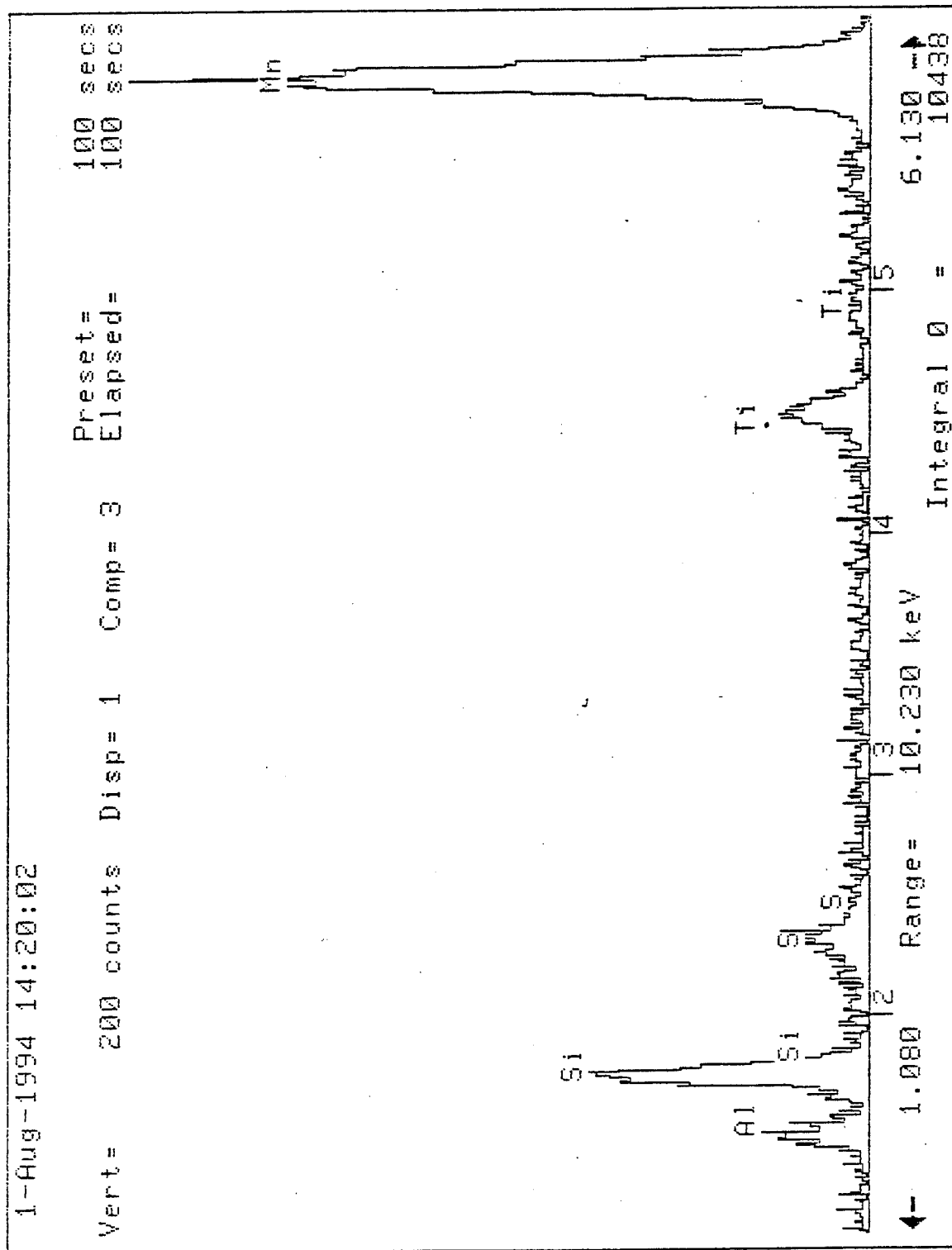
Figure B.03   Typical EDX   MV1

TABLE B.6 MV1 CHEMICAL OXIDE INCLUSION COMPOSITION

MV1:	GMAW	60 KJ/IN		C5 COVER	
		OXIDE/SULFIDE %			
	Al_2O_3	SiO_2	TiO_2	Cr_2O_3	MnO	MnS
1	2.00	16.60	11.59	0.0	58.86	10.96
2	0.84	21.20	2.83	0.0	67.80	7.34
3	1.55	17.34	2.16	0.0	43.50	35.44
4	0.43	26.24	1.80	0.0	68.71	2.82
5	2.47	18.66	3.44	0.0	65.90	9.54
6	2.56	18.05	3.22	0.0	62.40	13.78
7	1.95	19.60	10.98	0.0	58.50	8.98
8	4.50	20.42	8.25	0.0	61.17	5.66
9	3.64	18.47	7.58	0.0	58.79	11.52
10	2.57	19.07	10.09	0.0	61.07	7.20
11	4.67	20.80	6.34	0.0	60.62	7.56
12	3.44	16.61	4.42	0.0	53.17	22.36
13	5.77	20.06	4.02	0.0	57.57	12.58
14	4.81	22.84	1.78	0.0	47.18	22.76
15	3.69	18.96	8.18	0.0	51.73	17.46
16	0.68	21.84	2.92	0.0	63.69	10.86
17	5.24	21.99	5.31	0.0	49.55	17.92
18	3.87	19.13	10.27	0.0	58.11	8.64
19	6.09	13.04	19.29	0.0	46.56	15.02
20	5.05	20.28	7.42	0.0	57.36	9.92
AVE	3.29	19.59	6.59	0.0	57.61	12.92

TABLE B.7 MV2 CHEMICAL INCLUSION COMPOSITION

MV2: GTAW 60 KJ/IN ARGON COVER					
ATOMIC %					
	Al	Si	S	Ti	Cr	Mn
1	24.57	4.97	5.64	27.83	0.0	37.00
2	27.97	5.22	3.91	18.93	0.0	21.34
3	23.71	5.45	14.95	21.34	0.0	34.55
4	24.57	4.28	8.69	21.12	0.0	41.34
5	23.20	6.70	8.75	22.52	0.0	38.82
6	24.61	3.84	4.82	26.97	0.0	39.76
7	30.53	4.94	10.32	14.58	0.0	39.62
8	21.81	4.59	6.74	29.81	0.0	37.05
9	25.16	8.52	9.78	15.47	0.0	41.07
10	15.37	6.26	7.31	30.12	0.0	40.94
11	25.98	4.29	3.50	22.55	0.0	43.68
12	19.46	3.21	8.18	31.46	0.0	37.69
13	25.68	6.47	11.10	18.59	0.0	38.16
14	32.46	0.50	0.83	19.92	0.0	46.29
15	23.20	0.82	11.17	20.66	0.0	44.15
16	38.20	0.15	5.02	15.16	0.0	41.46
17	17.34	6.08	8.02	20.15	0.0	48.41
18	25.17	7.74	3.59	27.85	0.0	18.90
19	34.59	4.80	1.33	15.01	0.0	44.29
20	23.00	3.57	11.57	22.70	0.0	39.17
AVE	25.33	4.62	7.26	22.14	0.0	40.65
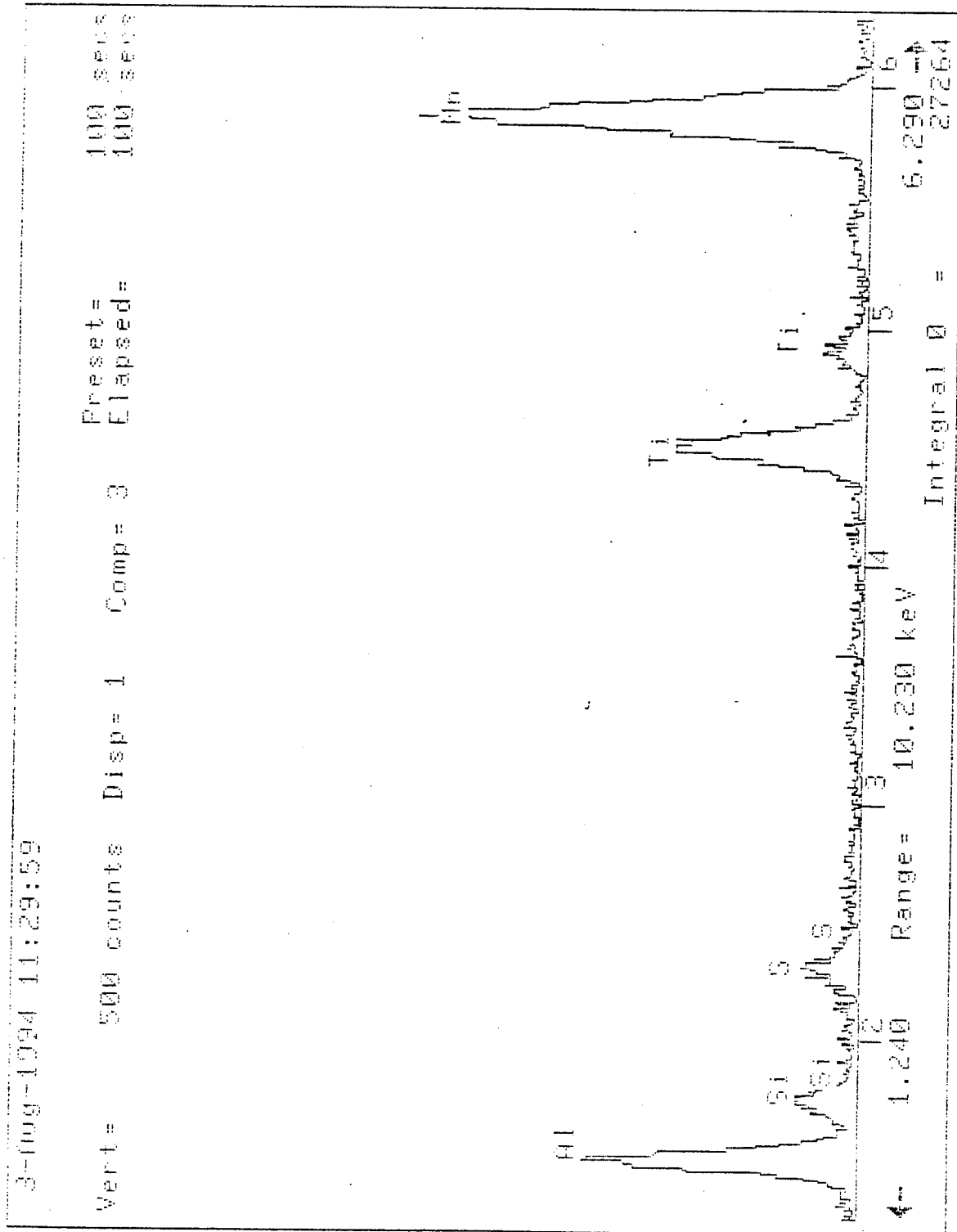
Figure B.04 Typical EDX MV2

TABLE B.8   MV2 CHEMICAL OXIDE INCLUSION COMPOSITION

MV2:	GTAW	60 KJ/IN		ARGON COVER		
			OXIDE/SULFIDE %			
	Al_2O_3	SiO_2	TiO_2	Cr_2O_3	MnO	MnS
1	18.28	4.36	32.46	0.0	31.72	13.18
2	21.34	4.69	22.63	0.0	41.96	9.38
3	17.55	4.76	24.75	0.0	18.20	34.74
4	18.35	3.77	24.72	0.0	32.76	20.40
5	17.29	5.89	26.31	0.0	30.03	20.48
6	18.33	3.37	31.48	0.0	35.56	11.26
7	23.38	4.46	17.51	0.0	29.81	24.84
8	16.02	3.98	34.34	0.0	30.11	15.56
9	19.07	7.61	18.37	0.0	31.67	23.28
10	11.10	5.33	34.11	0.0	32.86	16.60
11	19.59	3.81	26.64	0.0	41.68	8.28
12	14.11	2.75	35.77	0.0	28.72	18.64
13	19.32	5.73	21.91	0.0	26.82	26.22
14	24.97	0.45	24.01	0.0	48.56	2.00
15	17.12	0.71	23.90	0.0	32.39	25.88
16	29.91	0.14	18.61	0.0	39.00	12.34
17	12.75	5.27	23.22	0.0	40.25	18.52
18	18.90	6.85	32.77	0.0	33.02	8.46
19	27.13	4.44	18.45	0.0	46.72	3.26
20	16.98	3.11	26.26	0.0	26.83	26.82
AVE	19.07	4.07	25.91	0.0	33.93	17.02

TABLE B.9   MV3 CHEMICAL INCLUSION COMPOSITION

MV3: GTAW 78-161 KJ/IN C5 COVER					
ATOMIC %					
	Al	Si	S	Ti	Cr	Mn
1	31.14	8.14	3.35	9.65	1.81	45.91
2	34.13	6.76	3.29	8.80	1.66	45.35
3	30.06	8.49	7.41	9.03	1.37	43.63
4	37.43	6.08	4.71	6.55	1.12	44.11
5	38.68	5.79	2.84	5.94	1.21	45.55
6	33.34	9.86	1.90	7.51	1.85	45.54
7	25.11	16.81	3.82	6.70	1.07	46.49
8	30.41	11.23	2.32	7.69	1.62	46.72
9	29.35	7.36	3.20	9.89	1.04	49.16
10	47.05	4.95	2.36	5.01	1.78	38.84
11	36.00	6.51	3.71	7.65	1.94	44.19
12	29.52	8.77	6.12	7.56	1.94	46.09
13	30.94	10.45	3.21	5.84	2.51	47.05
14	34.06	7.48	2.37	7.33	1.19	47.54
15	25.53	12.24	3.98	7.34	1.05	49.85
16	20.74	19.88	3.45	6.41	0.38	49.14
17	23.28	21.18	2.60	5.80	0.73	46.40
18	25.60	20.18	1.90	6.97	0.0	45.36
19	4.60	24.49	5.37	2.29	0.62	62.63
20	3.37	28.87	6.41	0.83	0.0	60.52
AVE	28.52	12.28	3.72	6.74	1.24	47.50
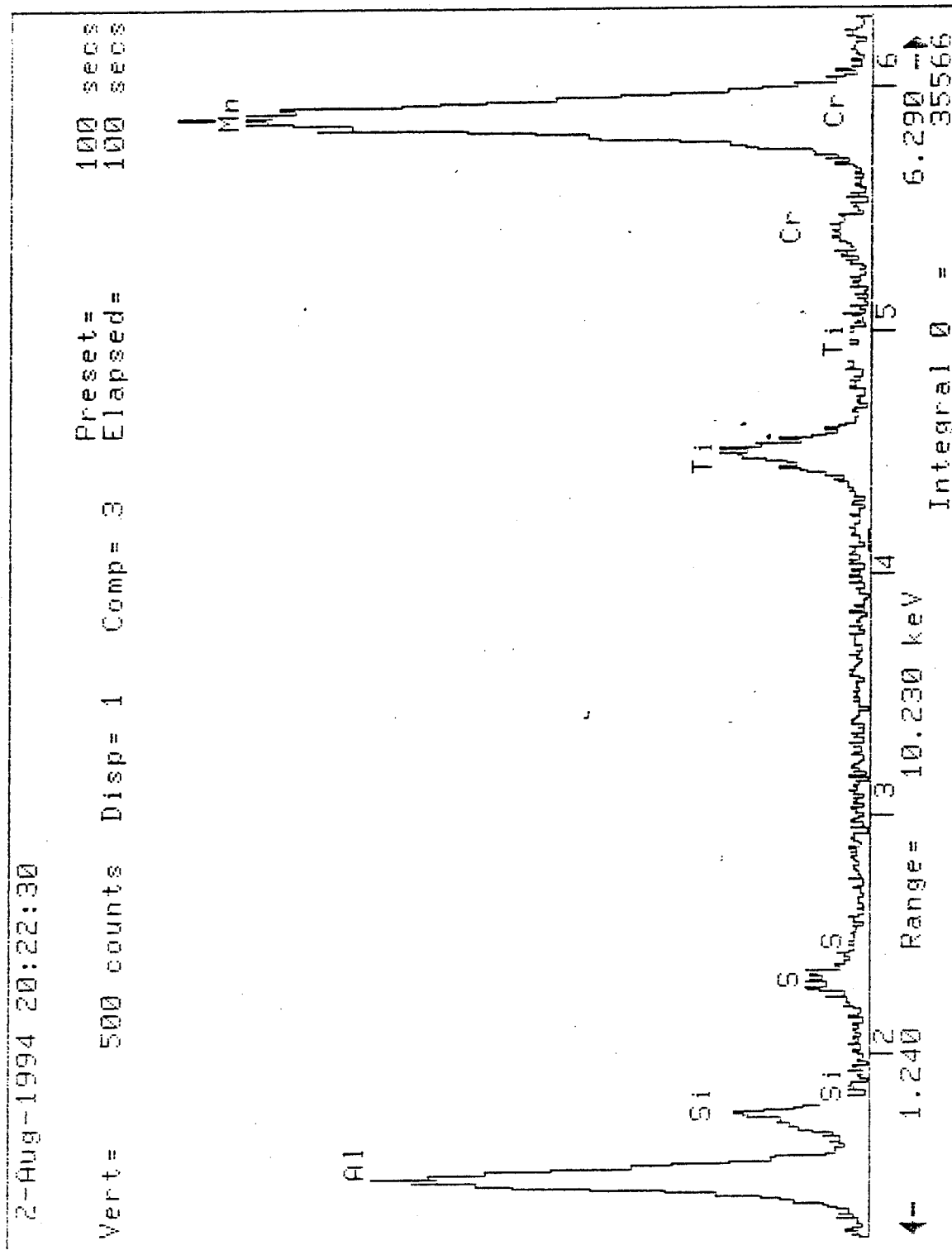
Figure B.05   Typical EDX   MV3

TABLE B.10   MV3 CHEMICAL OXIDE INCLUSION COMPOSITION

MV3:	GTAW	78-161 KJ/IN	C5 COVER		
OXIDE/SULFIDE %					
	Al_2O_3	SiO_2	TiO_2	Cr_2O_3	MnO	MnS
1	24.38	7.51	11.84	2.12	45.89	8.26
2	26.95	6.30	10.89	1.96	45.75	8.16
3	23.37	7.78	11.00	1.59	38.15	18.10
4	29.87	5.72	8.20	1.33	43.07	11.82
5	31.08	5.48	7.48	1.45	47.35	7.16
6	26.49	9.24	9.35	2.19	48.00	4.72
7	19.67	15.51	8.23	1.25	45.95	9.40
8	23.99	10.44	9.51	1.91	48.40	5.76
9	22.84	6.75	12.06	1.21	49.32	7.82
10	38.84	4.82	6.48	2.20	41.55	6.12
11	28.60	6.09	9.52	2.30	44.22	9.26
12	23.00	8.05	9.23	2.25	42.48	14.98
13	24.43	9.73	7.22	2.95	47.71	7.96
14	27.02	6.99	9.11	1.41	49.56	5.92
15	19.85	11.21	8.94	1.22	49.05	9.72
16	16.13	18.22	7.82	0.44	48.96	8.44
17	18.32	19.65	7.16	0.85	47.60	6.42
18	20.25	18.81	8.64	0.0	47.57	4.72
19	3.44	21.61	2.69	0.69	58.93	12.62
20	2.53	25.59	0.97	0.0	55.76	15.14
AVE	22.55	11.28	8.32	1.47	47.26	9.13

TABLE B.11   MV4 CHEMICAL INCLUSION COMPOSITION

| MV4:	GMAW	97 KJ/IN		C5 COVER	
ATOMIC %					
	Al	Si	S	Ti	Cr	Mn
1	4.13	22.47	11.86	2.67	0.0	58.87
2	4.10	24.98	6.19	2.18	0.0	62.55
3	4.68	25.18	7.82	1.36	0.0	60.95
4	4.23	22.27	8.60	1.40	0.0	63.50
5	4.01	23.92	5.49	5.35	0.0	61.23
6	5.65	19.17	5.83	8.57	0.0	60.78
7	3.28	21.84	3.80	7.00	0.0	64.08
8	2.56	26.64	5.64	2.98	0.0	62.19
9	3.84	21.24	7.75	4.57	0.0	62.60
10	4.81	22.23	5.27	5.12	0.0	62.57
11	3.64	23.02	5.06	3.02	0.0	65.27
12	4.57	24.46	2.78	6.53	0.0	61.66
13	4.40	25.13	6.53	6.23	0.0	57.70
14	3.71	27.19	6.48	2.45	0.0	60.17
15	3.55	25.59	6.06	1.97	0.0	62.83
16	3.22	22.90	7.31	3.98	0.0	62.60
17	2.47	24.19	6.47	5.18	0.0	61.70
18	2.61	22.93	9.86	2.50	0.0	62.10
19	4.56	18.07	8.03	7.37	0.0	61.96
20	3.38	24.96	3.35	4.14	0.0	64.16
AVE	3.87	23.42	6.51	4.23	0.0	61.97
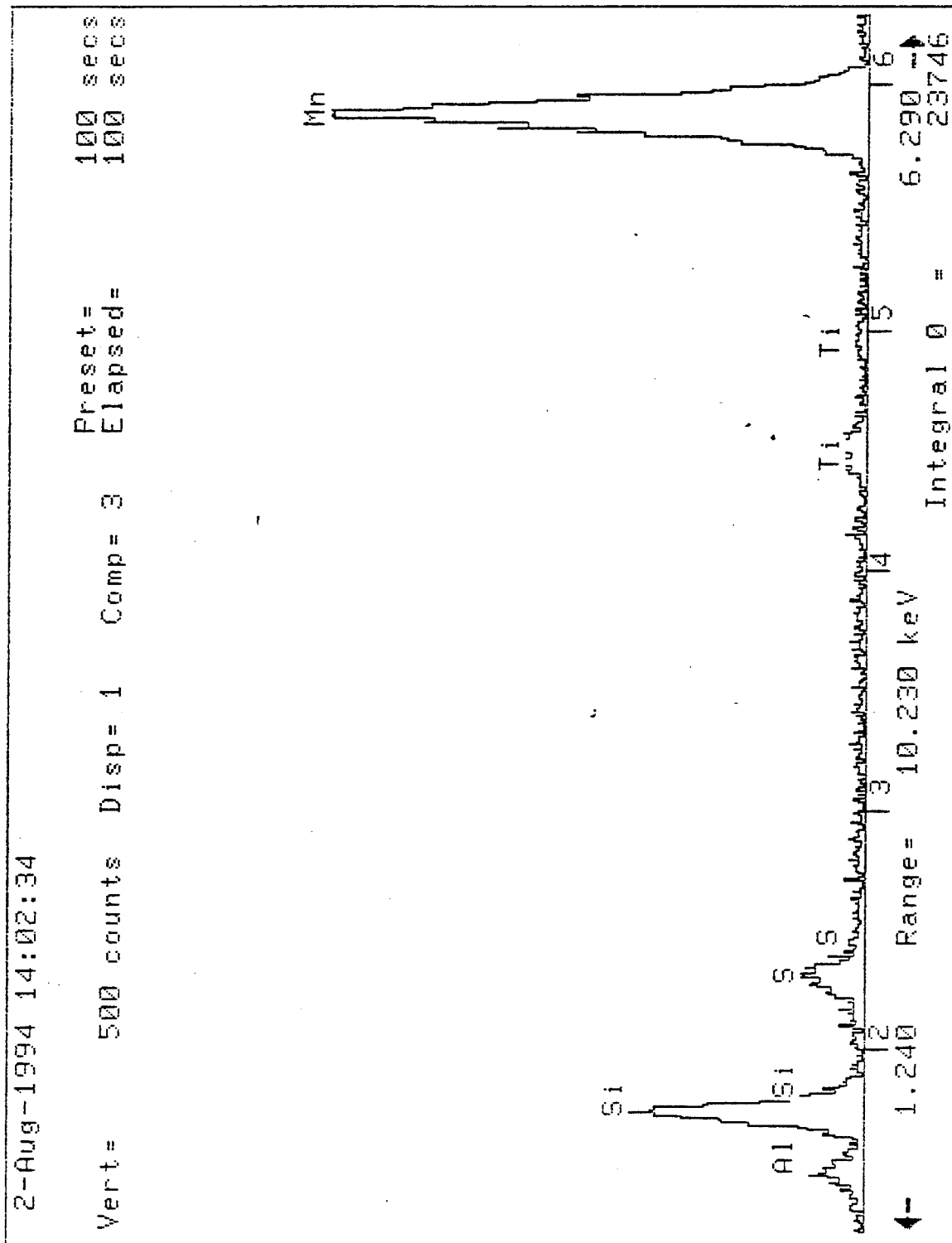
Figure B.06   Typical EDX   MV4

TABLE B.12   MV4 CHEMICAL OXIDE INCLUSION COMPOSITION

MV4: GMAW 97 KJ/IN C5 COVER					
OXIDE/SULFIDE %					
	Al_2O_3	SiO_2	TiO_2	Cr_2O_3	MnO	MnS
1	3.05	19.57	3.09	0.0	46.77	27.52
2	3.07	22.02	2.56	0.0	57.82	14.54
3	3.50	22.22	1.60	0.0	54.30	18.38
4	3.15	19.51	1.63	0.0	55.65	20.06
5	2.98	20.97	6.24	0.0	56.98	12.82
6	4.18	16.69	9.92	0.0	55.70	13.52
7	2.43	19.05	8.12	0.0	61.57	8.84
8	1.91	23.43	3.48	0.0	57.96	13.22
9	2.83	18.50	5.29	0.0	55.37	18.00
10	3.58	19.50	5.97	0.0	58.63	12.32
11	2.71	20.20	3.52	0.0	61.73	11.84
12	3.41	21.55	7.65	0.0	60.87	6.52
13	3.28	27.05	7.27	0.0	52.12	15.28
14	2.78	24.00	2.87	0.0	55.08	15.26
15	2.38	22.55	2.31	0.0	58.25	14.24
16	2.38	19.99	4.61	0.0	56.01	17.00
17	1.83	21.10	6.01	0.0	56.03	15.04
18	1.93	19.95	2.89	0.0	52.36	22.88
19	3.35	15.63	8.48	0.0	54.02	18.52
20	2.53	21.98	4.85	0.0	62.78	7.86
AVE	2.88	20.52	4.92	0.0	56.50	15.18

TABLE B.13   MV5 CHEMICAL INCLUSION COMPOSITION

MV5: GMAW 30 KJ/IN C5 COVER					
ATOMIC %					
	Al	Si	S	Ti	Cr	Mn
1	0.0	22.29	11.59	1.92	0.0	64.20
2	0.81	24.84	3.27	2.64	0.0	68.44
3	0.75	19.40	4.73	1.76	0.0	73.76
4	0.35	23.12	9.85	3.19	0.0	63.49
5	0.32	25.64	3.06	2.92	0.0	68.05
6	0.0	18.62	18.54	1.53	0.0	61.31
7	1.36	24.28	3.83	0.88	0.0	69.66
8	1.84	23.09	3.86	2.43	0.0	68.78
9	0.92	27.26	3.28	3.18	0.0	65.36
10	0.87	19.92	6.85	2.35	0.0	70.01
11	0.0	15.69	18.10	3.97	0.0	62.24
12	1.11	25.75	3.34	1.64	0.0	68.16
13	1.20	25.09	1.67	3.66	0.0	68.37
14	2.52	29.82	16.80	0.34	0.0	50.52
15	1.76	20.53	10.42	1.47	0.0	65.82
16	1.12	26.30	3.71	4.02	0.0	64.87
17	0.67	24.25	5.96	1.98	0.0	67.14
18	1.27	23.72	7.98	2.05	0.0	64.97
19	2.03	24.55	1.33	3.19	0.0	68.90
20	0.91	24.38	6.02	0.65	0.0	68.04
AVE	0.99	23.43	7.20	2.29	0.0	66.10
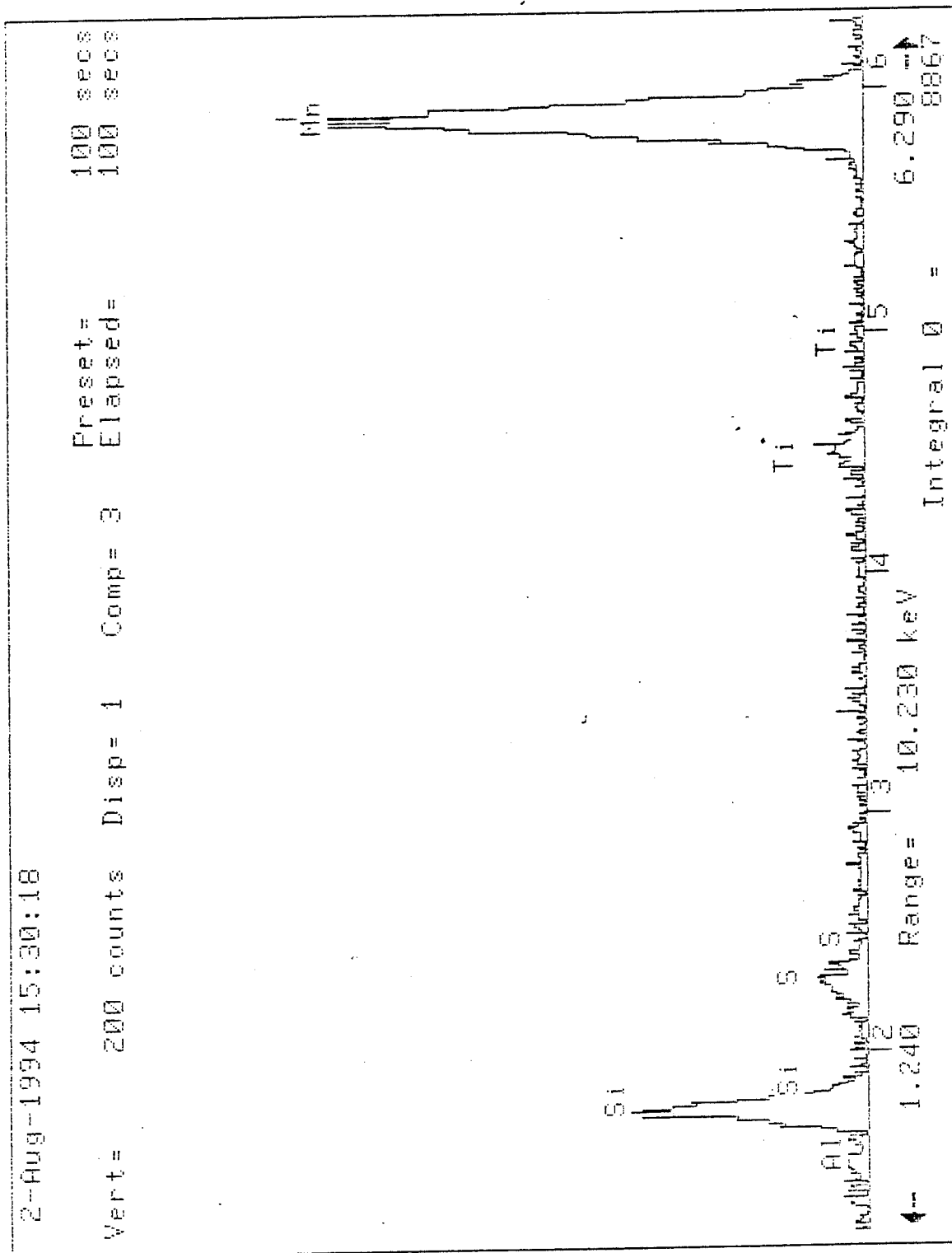
Figure B.07   Typical EDX   MV5

TABLE B.14 MV5 CHEMICAL OXIDE INCLUSION COMPOSITION

MV5: GMAW 30 KJ/IN C5 COVER					
OXIDE/SULFIDE %					
	Al_2O_3	SiO_2	TiO_2	Cr_2O_3	MnO	MnS
1	0.0	19.20	2.20	0.0	52.00	26.60
2	0.61	21.75	3.07	0.0	66.94	7.64
3	0.55	16.82	2.03	0.0	69.95	10.94
4	0.26	19.97	3.67	0.0	53.42	22.68
5	0.24	22.45	3.40	0.0	66.77	7.14
6	0.0	15.81	1.73	0.0	40.48	41.98
7	1.01	21.31	1.02	0.0	67.70	8.96
8	1.37	20.21	2.83	0.0	66.59	9.00
9	0.69	23.95	3.72	0.0	63.96	7.68
10	0.64	17.23	2.70	0.0	63.63	15.80
11	0.0	13.23	4.45	0.0	41.63	40.70
12	0.83	22.63	1.92	0.0	66.80	7.82
13	0.89	22.02	4.27	0.0	68.89	3.92
14	1.87	26.05	0.39	0.0	32.55	39.14
15	1.29	17.76	1.69	0.0	55.21	24.04
16	0.83	23.05	4.68	0.0	62.79	8.66
17	0.50	21.15	2.30	0.0	62.21	13.84
18	0.94	20.65	2.38	0.0	57.51	18.52
19	1.52	21.60	3.74	0.0	70.03	3.12
20	0.67	21.32	0.76	0.0	63.22	14.04
AVE	0.74	20.40	2.65	0.0	59.61	16.61

TABLE B.15   MV6 CHEMICAL INCLUSION COMPOSITION

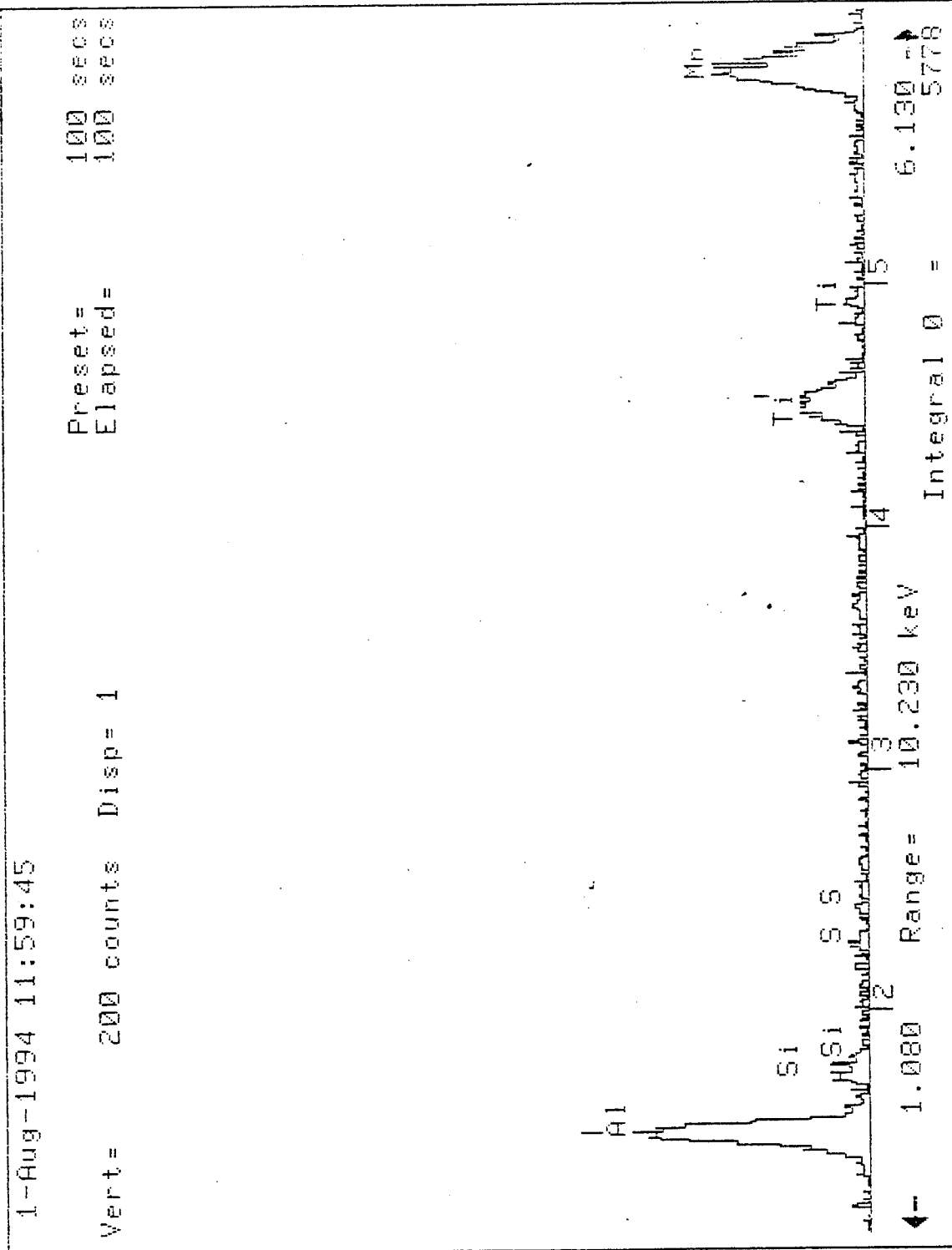| MV6: GMAW 60 KJ/IN ARGON COVER					
ATOMIC %					
	Al	Si	S	Ti	Cr	Mn
1	51.18	0.35	4.42	16.41	0.0	27.67
2	37.13	2.37	3.46	22.71	0.0	34.33
3	71.05	0.16	0.18	8.69	0.0	19.92
4	36.50	2.23	4.40	29.02	0.0	27.84
5	51.03	1.35	5.97	16.29	0.0	25.36
6	31.94	4.59	1.74	29.38	0.0	32.35
7	57.04	4.76	1.05	13.55	0.0	23.59
8	67.93	0.44	0.97	7.64	0.0	23.02
9	44.46	0.28	3.58	14.75	0.0	36.92
10	36.24	5.70	6.12	20.17	0.0	31.77
11	37.11	4.21	8.55	15.70	0.0	34.43
12	38.16	6.36	5.86	16.75	0.0	32.86
13	35.23	4.51	3.43	28.37	0.0	28.46
14	29.94	3.31	10.05	24.76	0.0	31.96
15	47.02	3.55	0.59	20.60	0.0	28.23
16	39.58	5.42	2.48	18.78	0.0	31.35
17	54.23	1.50	7.20	12.55	0.0	24.51
18	40.63	1.25	10.78	17.35	0.0	29.99
19	35.80	2.63	6.19	20.61	0.0	34.77
20	42.92	0.0	8.07	12.88	0.0	36.13
AVE	44.26	2.75	4.75	18.35	0.0	29.89

Figure B.08   Typical EDX   MV6

TABLE B.16 MV6 CHEMICAL OXIDE INCLUSION COMPOSITION

MV6: GMAW 60 KJ/IN ARGON COVER					
OXIDE/SULFIDE %					
	Al_2O_3	SiO_2	TiO_2	Cr_2O_3	MnO	MnS
1	41.70	0.33	20.96	0.0	25.69	11.30
2	28.84	2.17	27.66	0.0	32.89	8.44
3	62.96	0.17	12.07	0.0	24.32	0.48
4	28.02	2.02	34.91	0.0	24.43	10.61
5	41.55	1.30	20.79	0.0	21.09	15.28
6	24.36	4.13	35.11	0.0	32.23	4.18
7	48.19	4.74	17.94	0.0	26.33	2.80
8	59.60	0.45	10.50	0.0	26.78	2.66
9	35.59	0.27	18.51	0.0	36.63	9.00
10	28.23	5.23	24.62	0.0	26.94	14.98
11	28.99	3.87	19.22	0.0	26.94	20.98
12	30.09	5.91	20.70	0.0	28.80	14.50
13	27.10	4.09	34.20	0.0	26.33	8.28
14	22.53	2.93	29.20	0.0	21.59	23.74
15	38.01	3.38	26.10	0.0	31.01	1.50
16	31.35	5.06	23.32	0.0	34.10	6.18
17	44.79	1.46	16.24	0.0	18.82	18.68
18	31.76	1.15	21.25	0.0	19.38	26.46
19	27.68	2.40	24.98	0.0	29.90	15.04
20	34.05	0.0	16.02	0.0	29.83	20.10
AVE	35.77	2.55	22.72	0.0	27.20	11.76

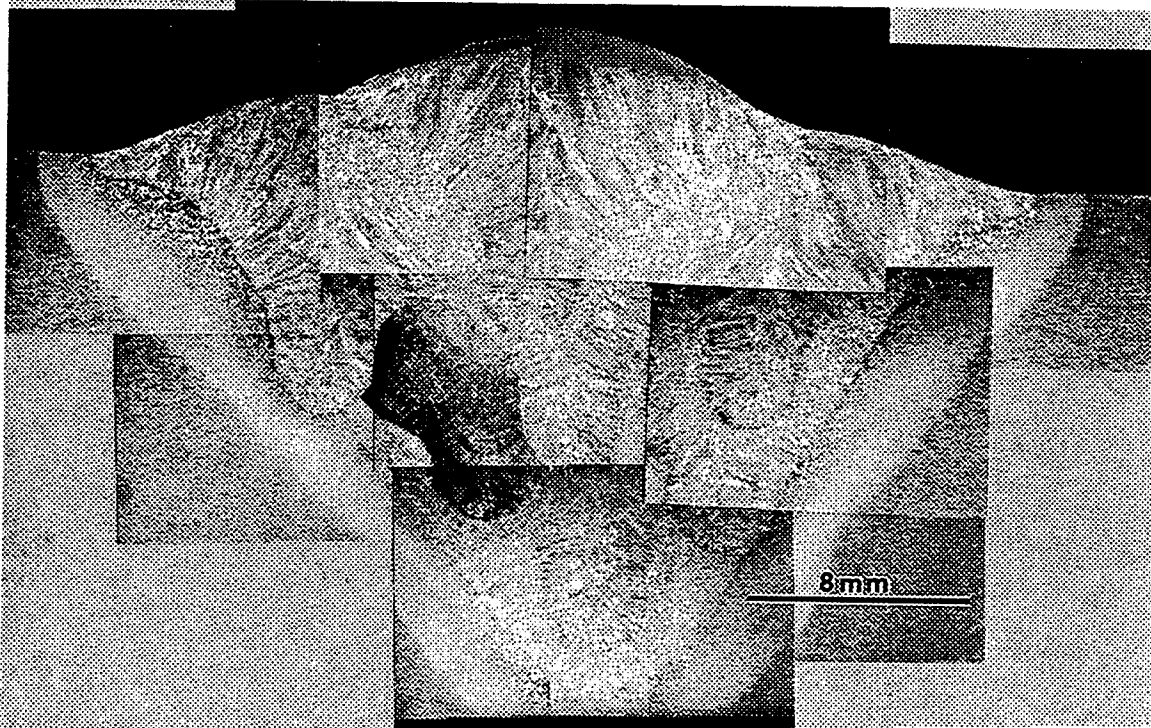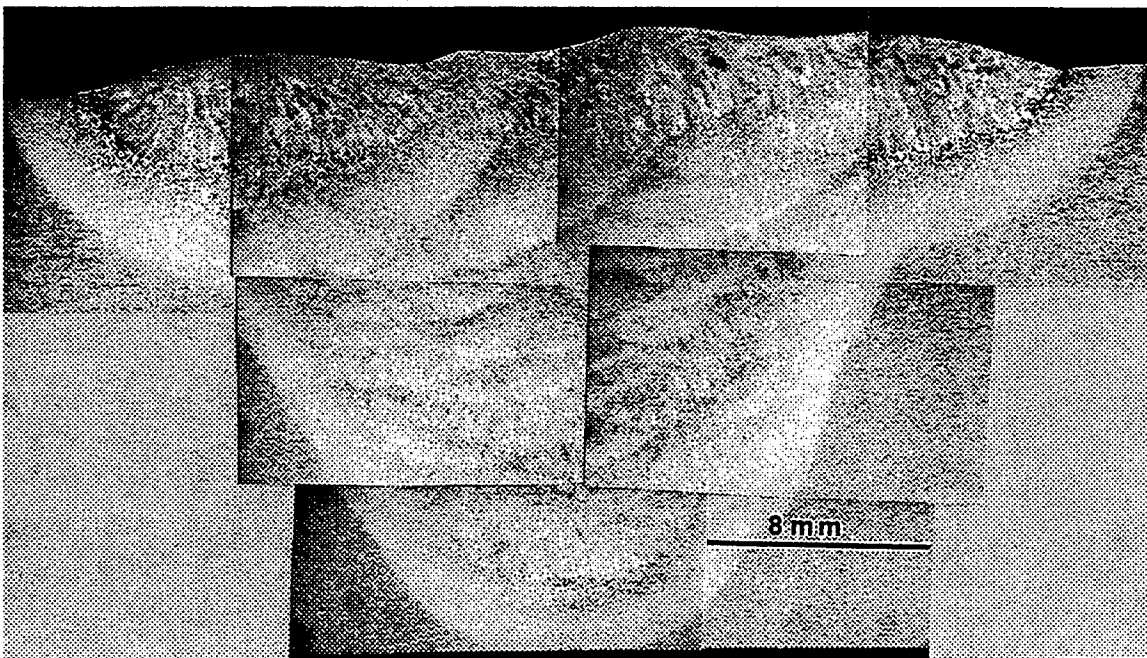## APPENDIX C OPTICAL MACROPHOTOGRAPHS
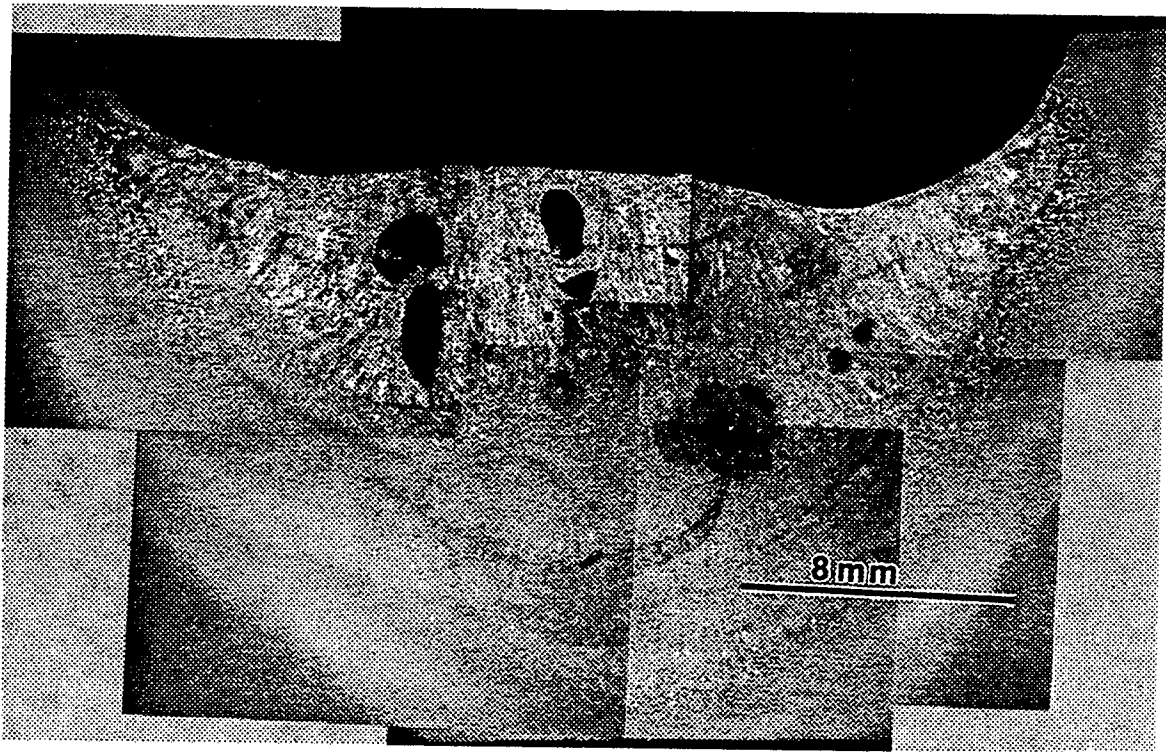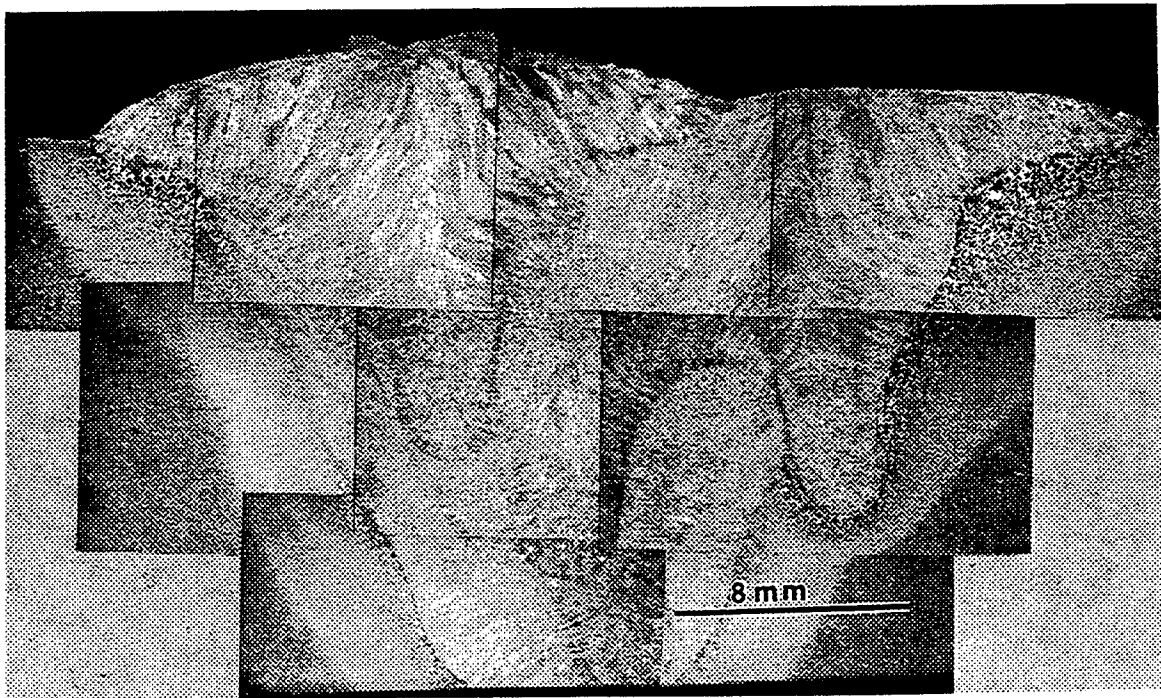

Figure C.1   MV1

Figure C.2   MV2

Figure C.3   MV3
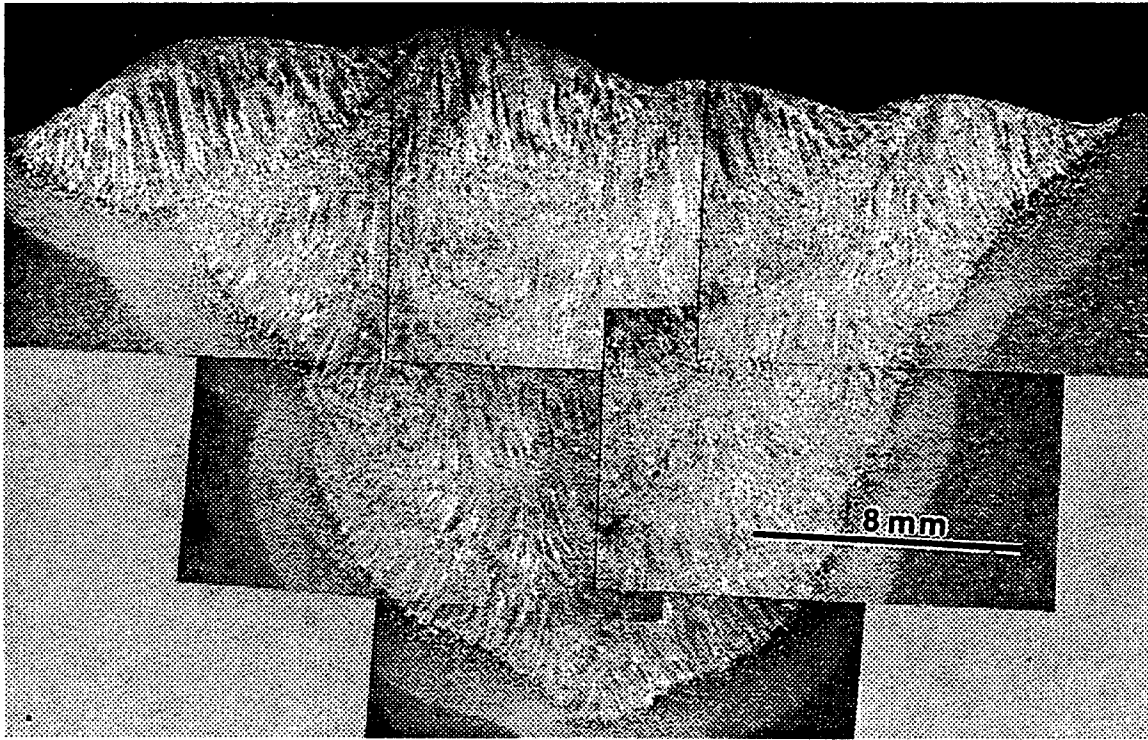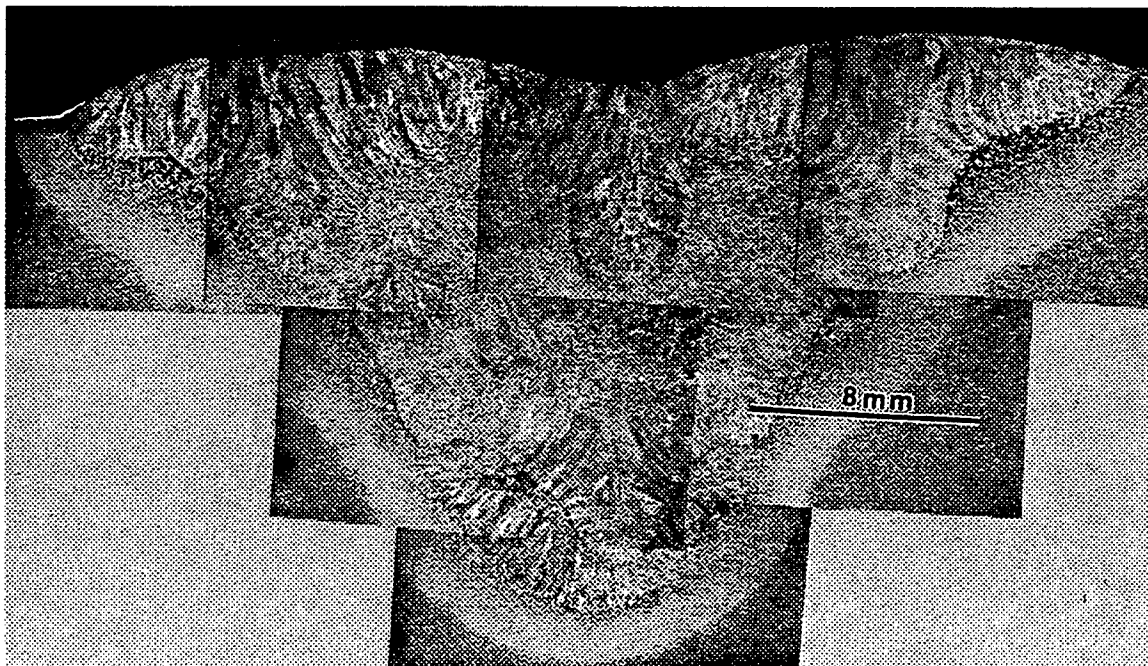

Figure C.4   MV4

Figure C.5   MV5

Figure C.6   MV6

LIST OF REFERENCES

Abson, D. J., Pargeter, R. J., Factors Influencing As-Deposited Strength, Microstructure, and Toughness of Manual Metal Arc Welds Suitable for C-Mn Steel Fabrications, International Metals Review, v.31, No. 4, 1986.

Blicharski, M. R., Garcia, C. I., Pytel, S., and De Ardo, J., Structure and Properties of ULCB Plate Steels for Heavy Section Applications, Processing, Microstructure and Properties of HSLA Steels, The Minerals, Metals and Materials Society, 1988.

Butler, D. E., The Quantitative Microstructural Characterization of Multipass TIG Ultra-Low Carbon Bainitic Steel Weldments and Correlation with Mechanical Properties, Master's Thesis, Naval Postgraduate School, Monterey, California, September 1993.

Callister, W. D. Jr., Materials Science and Engineering, John Wiley and Sons, 1991.

Chen, B., Zhou, Y., Improvement of Toughness and Strength of High Strength Steel Submerged Arc Weld Metal, China Weld Institute, 1988.

Czyrka, E. J., Link, R. E., Wong, R. J., Aylor, D. M., Montemarano, T. W., Gudas, J. P., Development and Certification of HSLA-100 Steel, Naval Engineers Journal, v. 102, no. 3, 1990.

Francis, R. E., Jones, J. E., Olson, D. L., Effect of Shielding Gas Oxygen Activity on Weld Metal Microstructure of GMA Welded Microalloyed HSLA Steel, Welding Journal 69, 1990.

Garcia, C. I., Lis, A. K., DeArdo, A. J., The Physical Metallurgy of Ultra-Low Carbon Bainitic Plate Steels, the Minerals, Metals and Materials Society, 1990.

Garcia, C. I., Lis, A. K., Pytel, S. M., DeArdo, A. J., Ultra-Low Carbon Bainitic Plate Steels: Processing, Microstructure and Properties, Iron and Steelmaker, 1991.

Graville, B. A., Proceeding Welding of HSLA (Microalloyed) Structural Steels (Roms), Metals Park, 1978.

Grong, O., Matlock, D. K., <u>Microstructural Developments in Mild and Low-Alloy Steel Weld Metals</u>, International Metals Review, 1986.

Hart, P. H. M., Hutt, G. A., <u>An Investigation Into the Factors Influencing Mechanized MIG Weld Metal Toughness</u>, The Welding Institute, 1987.

Kiessling, R., <u>Non-Metallic Inclusions in Steel</u>, The Metals Society, London, 1978.

Kou, S., <u>Welding Metallurgy</u>, John Wiley and Sons, 1987.

Lancaster, J. F., <u>Metallurgy of Welding</u>, Allen and Unwin, London, 1987.

McDonald, P. F. <u>Factors Influencing the Microstructure and Mechanical Properties of Ultra-Low Carbon Bainitic 100 Tungsten Inert Gas Multipass Weldments</u>, Master's Thesis, Naval Postgraduate School, Monterey, California, September 1992.

Okihito, S., Homma, H., Matsuda, S., Wakabayshi, M., Yamamoto, K., <u>Improvement of HAZ Toughness of HSLA Steel by Finely Dispersed Titanium Oxide</u>, Nippon Steel Technical Report (37), 1988.

Pickering, F. B., <u>Physical Metallurgy and the Design of Metals</u>, Applied Science Publishers, 1990.

Wang, F. F. Y., <u>Welding: Theory and Practice</u>, North-Holland, 1990.

Wilson, A. D., Hamburg, E. G., Clovin, D. J., Thompson, S. W., Kraus, G., <u>Properties and Microstructures of Copper Precipitation Aged Plate Steels</u>, Microalloyed HSLA Steels, Proceedings of Microalloying '88, ASM International.

Yang, J. R., Bhadeshia, H. K. D. H., <u>Thermodynamics of the Acicular Ferrite Transformation in Alloy-Steel Weld Deposits</u>, International Conference on Trends in Welding Research, ASM International, 1989.

Zhou, Z. L., Norinder, H., <u>Influence of Microstructure on Fracture Toughness of Weld Metals</u>, International Journal for the Joining of Metals, 1993.

INITIAL DISTRIBUTION LIST

		No. Copies
1.	Defense Technical Information Center Cameron Station Alexandria, Virginia 22304-6145	2
2.	Library, Code 52 Naval Postgraduate School Monterey, California 93943-5101	2
3.	Naval Engineering Curricular Office, Code 34 Naval Postgraduate School Monterey, California 93943	1
4.	Department Chairman, Code ME Department of Mechanical Engineering Naval Postgraduate School Monterey, California 93943	1
5.	Dr. Alan G. Fox, Code ME/FX Department of Mechanical Engineering Naval Postgraduate School Monterey, California 93943	2
6.	Dr. Michael G. Vassilaros Naval Surface Warfare Center Carderock Division, Annapolis Detachment Code 615, 3A Leggett Circle Annapolis, Maryland 21402-5067	1
7.	LT Michael L. Beno 1226 Calle Del Lago Socorro, New Mexico 87801	2